



Digitized by the Internet Archive
in 2019 with funding from
University of Alberta Libraries

<https://archive.org/details/interactionofsur00clau>

THE UNIVERSITY OF ALBERTA

INTERACTION OF SURFACTANTS ON
FLOTATION OF METALS AND MINERALS

A Thesis

Submitted to the Faculty of Graduate Studies
in Partial Fulfilment of the Requirements
for the Degree of Master of Science

by

CLAUDIO GUARNASCHELLI

DEPARTMENT OF MINING AND METALLURGY

EDMONTON, ALBERTA

MARCH, 1965

UNIVERSITY OF ALBERTA
FACULTY OF GRADUATE STUDIES

The undersigned certify that they have read and recommend to
the Faculty of Graduate Studies for acceptance, a thesis titled

INTERACTION OF SURFACTANTS ON FLOTATION OF METALS AND MINERALS

Submitted by CLAUDIO GUARNASCHELLI
in partial fulfilment of the requirements for the degree of Master of
Science.

ABSTRACT

Adsorption kinetics of xanthates from aqueous solutions has suggested a comprehensive mechanism of adsorption. Xanthate anions as such do not adsorb on a metal surface and are readily oxidized to dixanthogen or complexed with $C_{12}TAB$ to form a neutral molecule. It is postulated that this neutral molecule transports the xanthate anion to the surface where it is readily chemisorbed. At first adsorption occurs at the available active sites of the metal surface but, as soon as they are occupied, other sites are activated and the process continues, this time enhanced by the simultaneous formation of xanthate crystallites. The final adsorption step is limited to the growth of the crystallites.

ACKNOWLEDGEMENT

The author is extremely grateful to Dr. J. Leja for his valuable guidance and suggestions regarding the theoretical interpretation of this investigation.

Appreciation is expressed to Dr. R.V. Scowen for the continued interest and discussions on all of the topics of this work and to Dr. W.V. Youdelis for his assistance in the interpretation of reaction rate data.

The technical assistance of many members of the Department of Mining and Metallurgy, particularly of Mr. J. Wojno and the indomitable endurance of my wife in typing this thesis have been appreciated.

Grateful acknowledgement is made to the Consolidated Mining and Smelting Company of Canada Limited for receiving a generous financial assistance.

CHEMICAL NOTATION AND DATA ON COMPOUNDS USED

Abbreviated Form	Name	Formula	Molecular Weight
C ₁₂ TAB	dodecyl trimethyl ammonium bromide	C ₁₂ H ₂₅ (CH ₃) ₃ N ⁺ Br ⁻	308.361
C ₁₈ TAB	octadecyl trimethyl ammonium bromide	C ₁₈ H ₃₇ (CH ₃) ₃ N ⁺ Br ⁻	392.523
KEtX	potassium ethyl xanthate	CH ₃ CH ₂ OC ⁼ _{SK} S	160.305
KC ₆ X	potassium hexyl xanthate	CH ₃ (CH ₂) ₅ OC ⁼ _{SK} S	216.413
KC ₉ X	potassium nonyl xanthate	CH ₃ (CH ₂) ₈ OC ⁼ _{SK} S	258.494
Stearic acid	octadecanoic acid	CH ₃ (CH ₂) ₁₆ COOH	284.47
Heptane	heptane	CH ₃ (CH ₂) ₅ CH ₃	100.20

TABLE OF CONTENTS

	Page
INTRODUCTION	
Theories of Adsorption	1
Electrical Phenomena at Interfaces	3
IDENTIFICATION OF REACTANTS USING UV SPECTROSCOPY	7
Theory	7
Spectra of KETX and $C_{12}TAB$	9
EXPERIMENTAL	13
Materials	13
Apparatus	15
Procedure in Systems Open to the Atmosphere	17
Procedure in Systems under a Nitrogen Atmosphere	18
Testing Program and Results	19
DISCUSSION	31
Stoichiometry of the Reaction	31
Studies of Mixtures of Xanthates and C_nTAB	32
a) Chemical composition	33
b) X-ray diffraction	33
Role of Intermediates in Organic Reactions	38
Reaction Order	41
Activation Energy as a Criterion of Mechanism	47
Role of Gases in Adsorption Studies	55
Evaluation of Results	60
SUMMARY AND CONCLUSIONS	63
REFERENCES	66
APPENDIX A	68
Surface Area Measurements	69
APPENDIX B	73
Detailed Analysis of Test No. 17	75
Detailed Analysis of Test No. 16	77
Least Squares Analysis of Test No. 16	78
Standard Deviation (Standard Error)	79
APPENDIX C	81
Activation Energy	82
Entropies of Activation	84

LIST OF TABLES

		Page
TABLE I	Beer's law for potassium ethyl xanthate	12
TABLE II	Basic testing program	21
TABLE III	Percentage composition of KC_6X , $C_{18}TAB$ (calculated from exact formula) and the corresponding precipitate from an equimolar mixture of the two (actual assay and calculated 1:1 ratio)	34
TABLE IV	Percentage composition of KC_9X , $C_{12}TAB$ (calculated from exact formula) and the corresponding precipitate from an equimolar mixture of the two (actual assay and calculated 1:1 ratio)	35
TABLE V	X-ray diffraction data	36
TABLE VI	General scheme of influence of dissolved gases on flotation	57
TABLE VII	Detailed analysis of test number 17	75
TABLE VIII	Detailed analysis of test number 16	77

LIST OF FIGURES

	Page
Fig. 1 Beer's law for potassium ethyl xanthate using a 1mm quartz cell	11
Fig. 2 Arrangement of the adsorption apparatus	16
Fig. 3 Adsorption of KEtX and mixture of KEtX and $C_{12}TAB$ on 10g of copper (not reduced) in systems open (-) and closed (--) to the atmosphere at $10^{\circ}C$	22
Fig. 4 Adsorption of KEtX and mixture of KEtX and $C_{12}TAB$ on 10g of copper (reduced) in systems open (-) and closed (--) to the atmosphere at $10^{\circ}C$	23
Fig. 5 Adsorption of KEtX and mixture of KEtX and $C_{12}TAB$ on 6g of copper (reduced: -- and not reduced: -) in a system open to the atmosphere at $10^{\circ}C$	24
Fig. 6 Adsorption of KEtX and mixture of KEtX and $C_{12}TAB$ on 1.8g of copper (reduced: -- and not reduced: -) in systems open (-) and closed (--) to the atmosphere at $10^{\circ}C$	25
Fig. 7 Adsorption of KEtX and mixture of KEtX and $C_{12}TAB$ on 10g of copper (not reduced) in systems open (-) and closed (--) to the atmosphere at $4^{\circ}C$	26
Fig. 8 Adsorption of KEtX and mixture of KEtX and $C_{12}TAB$ on 10g of copper (reduced) in systems open (-) and closed (--) to the atmosphere at $4^{\circ}C$	27
Fig. 9 Adsorption on the apparatus and decomposition of KEtX and $C_{12}TAB$ in tests with and without sphalerite at $10^{\circ}C$ in a nitrogen atmosphere	28

Fig. 10	Adsorption on the apparatus and decomposition of KEtX and $C_{12}TAB$ in tests with and without sphalerite at $4^{\circ}C$ in a nitrogen atmosphere	29
Fig. 11	Adsorption on apparatus and decomposition of KEtX and $C_{12}TAB$ at different temperatures in systems open and closed to the atmosphere	30
Fig. 12	Proposed head-to-head arrangement of the precipitates formed from equimolar mixtures of $C_{18}TAB$ with KC_6X and $C_{12}TAB$ with KC_9X	37
Fig. 13	Graphical representation of zero, first, second and third order reactions for KEtX in a test on copper powder at $10^{\circ}C$ in a system open to the atmosphere	43
Fig. 14	Effect of a change in xanthate concentration on adsorption of KEtX from a solution of KEtX on 10g of copper (not reduced) in a system open to the atmosphere at $10^{\circ}C$	45
Fig. 15	Effect of a change in xanthate concentration on adsorption of KEtX from a mixture of KEtX and $C_{12}TAB$ on 10g of copper (not reduced) in a system open to the atmosphere at $10^{\circ}C$	46
Fig. 16	Adsorption of KEtX on 10g of copper (not reduced) from a solution of KEtX in a system open to the atmosphere	52
Fig. 17	Adsorption of KEtX on 10g of copper (reduced) from a mixture of KEtX and $C_{12}TAB$ in a nitrogen atmosphere	53
Fig. 18	Temperature independence of Arrhenius activation energy for KEtX from a solution of KEtX alone in a system open to the atmosphere (A) and for KEtX from an equimolar solution of KEtX and $C_{12}TAB$ in nitrogen atmosphere (B)	54
Fig. 19	Influence of various gases on adsorption of a mixture of KEtX and $C_{12}TAB$ on 10g of copper (reduced) at $10^{\circ}C$	59

Fig. 20	Adsorption isotherm for stearic acid on copper powder at 20°C	72
Fig. 21	Test No. 17	74
Fig. 22	Test No. 16	76

INTRODUCTION

Froth flotation relies on the selective adsorption of heteropolar molecules from an aqueous solution and the subsequent formation of an hydrophobic film at the liquid/solid interface. The bond strength between the adsorbed species and the substrate may vary from a strong covalent (e.g. xanthates) to a weak electrostatic attraction (e.g. amines), with additional van der Waals attractions between hydrocarbon chains acting as contributory lateral bonds. Studies of the adsorption from mixed surfactants solutions are of primary interest since the adsorption kinetics and mechanism may be different from the ones operative when only one species is present.

Once the mechanism and the kinetics of the reaction are evaluated, it is feasible that an entirely new approach to the flotation of mixed minerals may be applied. Bowcott²⁴ noticed that xanthates appear to be stabilized against atmospheric oxygen at the air/liquid interface by alcohol and quaternary ammonium compounds. Buckenham and Schulman²³ observed that a 1:1 ratio between xanthate and C₁₆TAB produced a greater reduction in surface tension than solutions of the individual ions and proposed that adsorption of the complex can occur on either positively or negatively charged solids.

Subsequent work carried out in this Department by Pomianowski and Leja²² suggested that the initial interpretation given by Buckenham and Schulman²³ needed more confirmatory evidence on the following points: a) the extent of these molecular associations;

b) whether associations take place at the air/liquid interface and/or in the bulk of the solution; c) preferential adsorption of the individual molecules compared to the adsorption of the molecular complex. The primary objectives of this work were to investigate the basic aspects of adsorption and adsorption kinetics with the aim of further extending the work of Pomianowski and Leja²². Added evidence is presented on the ability of the C₁₂TAB to allow the adsorption of KEtX in anaerobic systems.

Theories of Adsorption

Heavy metal xanthates are fairly insoluble in water suggesting that xanthate chemisorption may occur at the solid/liquid interfaces of corresponding metals or metal sulphides. Films of lead ethyl xanthate have been identified on galena surfaces by Hagiwara¹ using electron diffraction technique and similarly, mixed films of cuprous ethyl xanthate and dixanthogen on copper (and lead ethyl xanthate on galena) have been identified by Poling² with the use of IR reflectance technique. Alkali metal xanthates are very soluble (2-5M), lead and zinc xanthates are more insoluble (solubility products: $\sim 10^{-15}$ - 10^{-10}) but the most insoluble of all are the copper, silver, gold and mercury xanthates (solubility products: $\sim 10^{-40}$ - 10^{-20})³. The above sequence indicates that chemical bonds between the xanthate group and the metal may vary from highly ionic to covalent. This relative bond strength

is the basis of the adsorption theories of xanthates.

Taggart⁴ advanced a chemical theory of adsorption based on the idea of relative solubility. The product formed on adsorption of xanthate ion to the metal-containing substrate must be more insoluble than the mineral surface or any other alteration product present on the same surface. The limitations and difficulties of Taggart's theory have been discussed by Sutherland and Wark⁵ and Gaudin⁶ who proposed that xanthates, in general, are adsorbed on a sulphide mineral by exchange of ions in the double layer. This modification was necessary because some of the mineral surfaces were more insoluble than the corresponding metal xanthates. This modified form of the chemical theory, called the "Ion Exchange Theory", is perhaps the most widely accepted version.

Recently, Cook et al^{7,8} advanced the non-ionic "Free Acid Theory" to account for the electrical neutrality of the surface. However, no mention is made of any further adsorption or dissociation of this xanthic acid.

In comparison with the chemisorption of xanthates, the adsorption of amines and derivatives is physical in character. Gaudin and Bloecher⁹ investigated the attachment of dodecylamine on quartz by replacement of radioactive amine with unmarked amine and stated that "At any one instant, for a given concentration of dodecylamine acetate in solution, there is a certain total amount of dodecylamine on the quartz surface. The individual dodecylamine chains, however, are not firmly anchored there. They are continually arriving and departing from the surface. At equilibrium, the rate

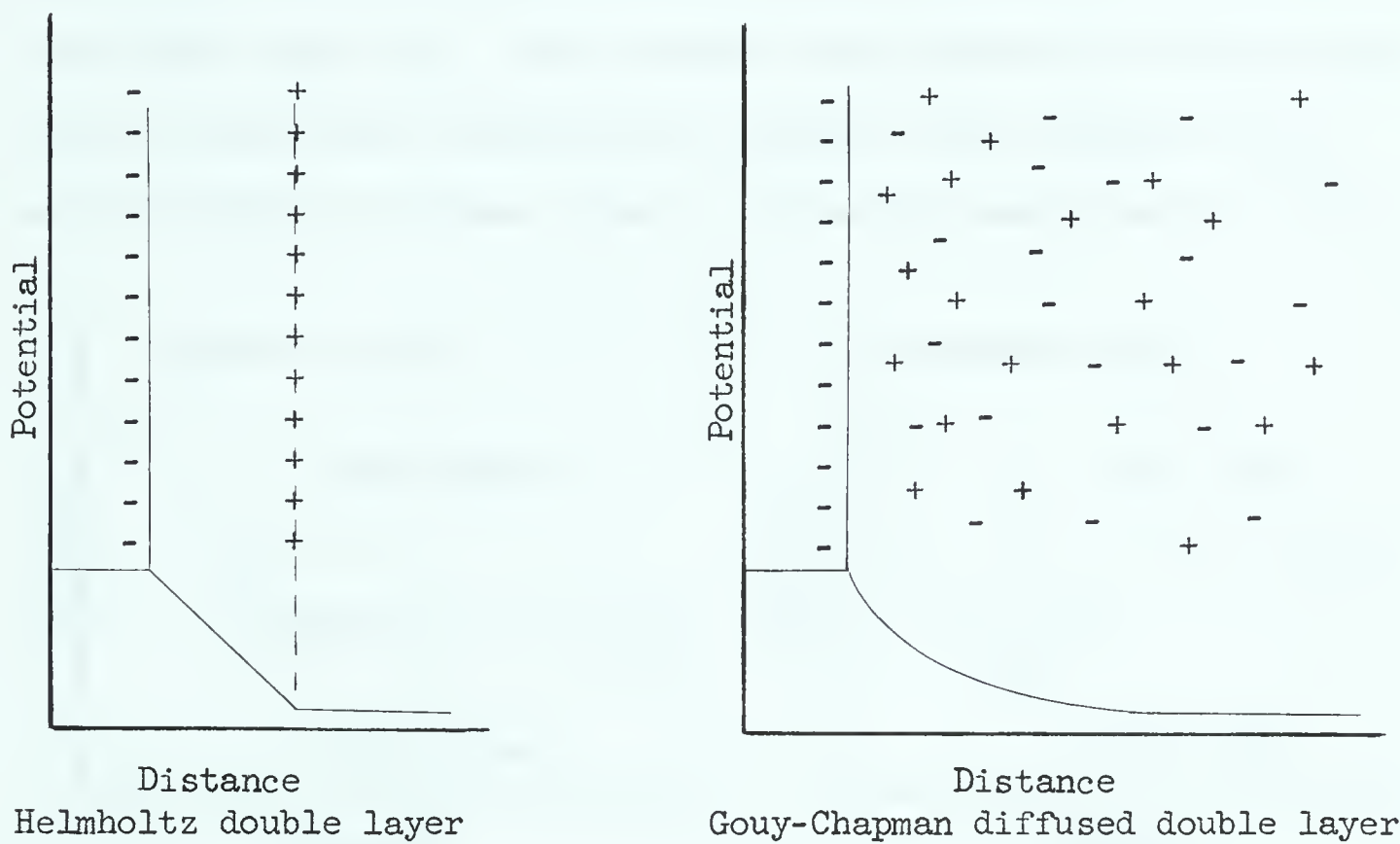
of adsorption from solution is equal to the rate of desorption."

Moreover, the amount adsorbed from solution was found to be less than 5% of the amount required to complete a monolayer. Fuerstenau¹⁰ following the same captive bubble technique used by Gaudin and Morrow¹¹ correlated surface phenomena at the solid/liquid interface (adsorption density and zeta potentials) with surface phenomena at the solid/liquid/gas interface (contact angle and flotation experiments). The association of collector ions in the Stern layer and its relation to the sign of the surface charge has been stressed by Fuerstenau and Modi¹². If the surface charge is negative, cationic collectors will float the mineral, if positive anionic collectors will be used to achieve the same results. Apart from electrical charge considerations, ionic size and chemical properties (hydrolysis) play an important role in adsorption. Ionic size determines how strongly an ion is adsorbed in the Stern layer and the extent of ion hydration. The size of the charged group of the quaternary ammonium compounds is so large that adsorption is definitely lessened. The length of the hydrocarbon chain and the presence of double bonds in the non-polar chain control the association of adsorbing collectors ions, the insolubility and the tendency to associate in the Stern layer (Purcell G.¹³).

Electrical Phenomena at Interfaces

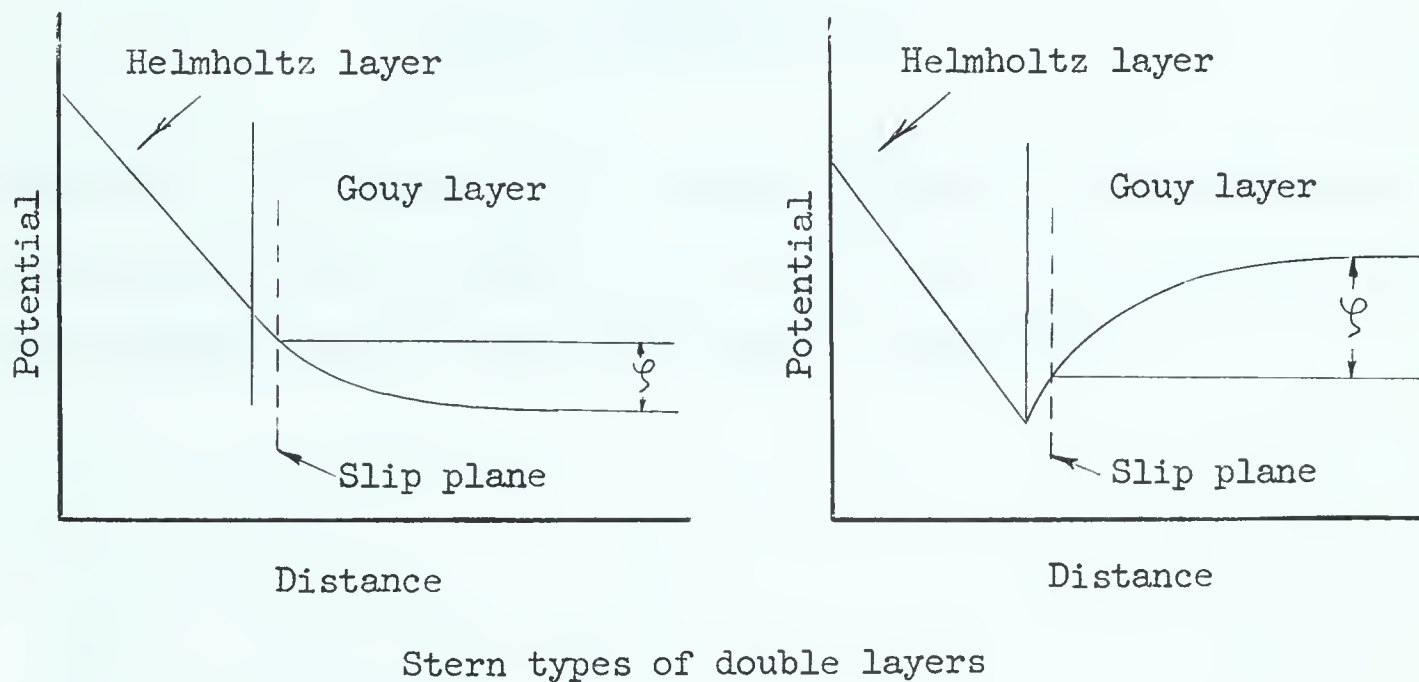
The existence of a potential difference across an interface implies that there is an unequal distribution of charges in the two phases but the condition of electrical neutrality for any phase suggests that the potential difference occurs almost at the phase

boundary. The first model of this electrical double layer is due to Helmholtz¹⁴ who proposed that a uniformly distributed potential difference existed between two layers of point charges of opposite sign, each layer residing in the respective phases. The solid (metal or metal sulphide) immersed in water takes up a negative charge due to dissolution of metal cations leaving behind free electrons.

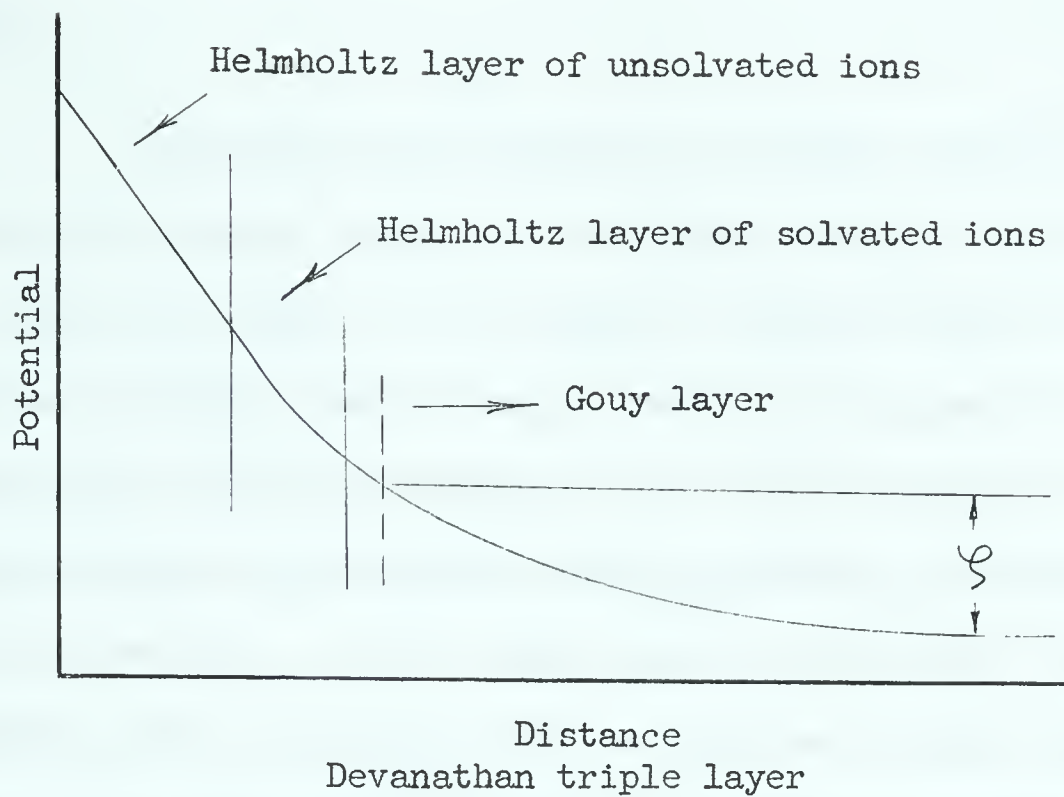


The capacity of the electrical double layer varies with the potential difference across the metal/electrolyte and with the nature and concentration of the electrolyte. To explain these effects and the fact that the charges in the solution phase would attract opposite charges available in solution, thus causing a disturbance of the bulk charges, Gouy¹⁵ and Chapman¹⁶ suggested that the electrical double layer has a diffuse structure. They were able, then, to calculate the total charge density in terms of the concentration and potential difference but the calculated variation of the double-layer capacity was greater

than the one actually observed. An improved model taking account of ionic sizes of charges and specific adsorption was proposed in 1924 by Stern¹⁷. Thus the electrical double layer is a combination of the Helmholtz and diffuse layers and, therefore, the total charge density is equal to the sum of the charge densities for the Helmholtz and diffuse components. The capacity of the Stern double layer, C_s , is calculated from the capacities of the Helmholtz layer, C_h , and diffuse double layer, C_d . The potential drop between the bulk solution and the slip plane (separating the immobile film attached to the solid) within the diffuse layer is called the zeta potential (ζ).



Grahame¹⁸ used the calculated values of C_d and was able to demonstrate that the total double layer capacity depends mainly on the capacity of the Helmholtz component and ionic solvation in the double layer. Following these lines of thought, Devanathan¹⁹ proposed a triple layer consisting of two Helmholtz layers of unsolvated and solvated ions and a diffuse Gouy layer.

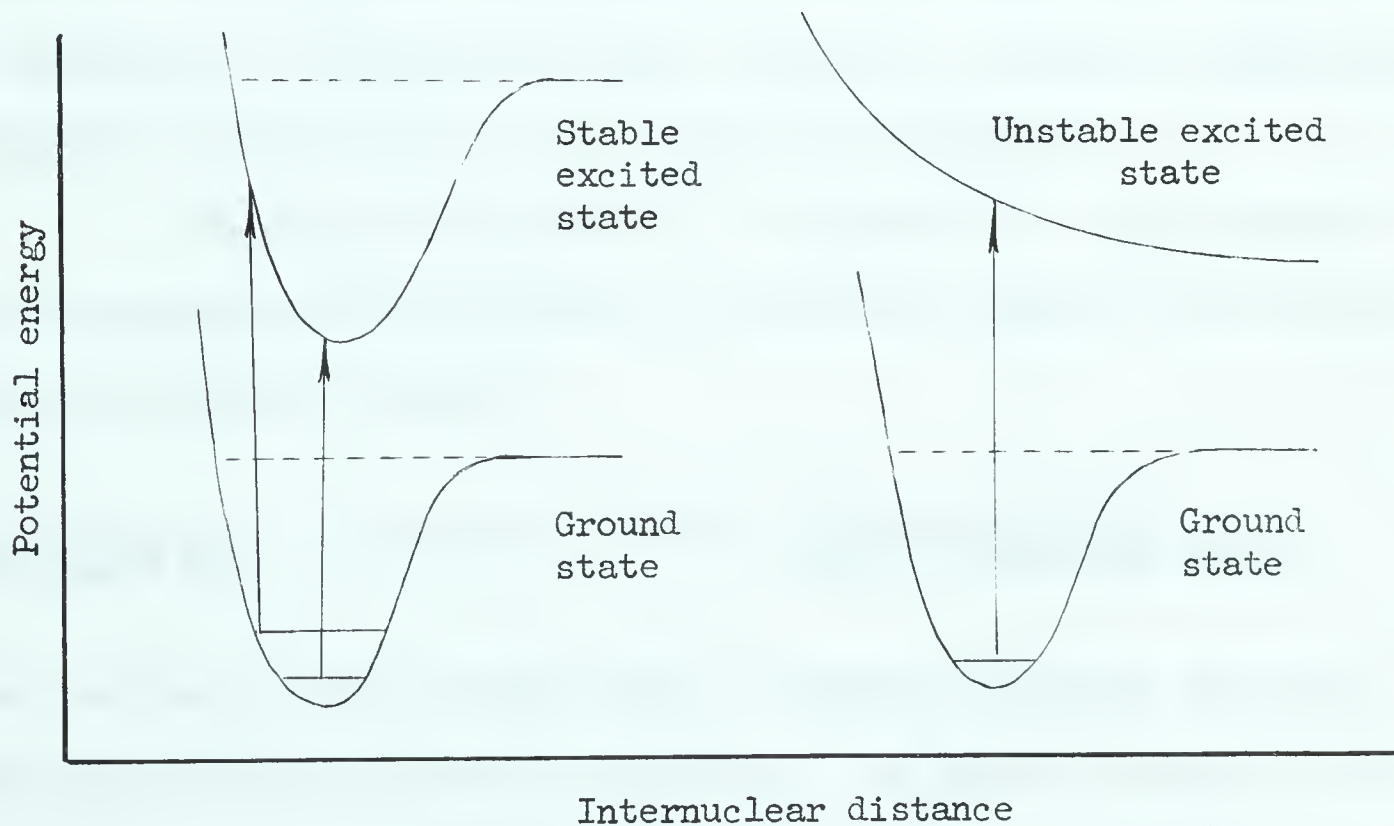


The lack of information on the extent of hydration of the adsorbed ions precludes any treatment of the triple layer model of Devanathan and the Stern model of the double layer is being used.

IDENTIFICATION OF REACTANTS USING UV SPECTROSCOPY

Theory

Absorption spectroscopy is directly concerned with absorption of radiant energy by a molecule causing a transition between two electronic states. If we analyze a chemical bond in terms of the familiar potential energy diagram (one of the curves for the ground state in the following diagram) we see that two atoms at infinite distance possess considerable potential energy, the potential energy of bond formation. As the atoms approach each other, the nuclei attraction assumes importance and the potential energy reaches a minimum, then, as the internuclear distance is reduced, repulsive forces become predominant and the potential energy curve rises steeply. Molecules in their electronic ground state can be promoted into an electronically excited state by absorption of light of appropriate frequency²⁰.



When a molecule is electronically excited (one or more valence electrons in a metastable orbital) it possesses more potential energy than a molecule in the ground state. This molecule can be found in either a stable or unstable excited state. Such a transition is possible because the energy difference between two electronic states in a molecule is, in general, much larger than the one between successive vibrational levels. The promotion of electrons to higher orbitals occurs more quickly than the period of vibration of the atomic nuclei (approximately 10^{-13} sec) which are heavy and sluggish compared to electrons (Frank-Condon principle). In the ground state a transition will occur from the midpoint of the vibration, where we have the maximum probability of finding an electron, but for higher vibrational levels this principle does not apply because the maximum probabilities lie closer to the extremes of the vibration and, therefore, a transition will take place from one of those points. Different molecules, then, will display an absorption of energy of different frequency to induce the particular transition characteristic of each molecular arrangement.

Spectrum wavelengths (λ), frequency (ν), and wavenumber are frequently used in reference to a particular region of the spectrum. They are related as follows:

$$\frac{1}{\text{Wavelength (cm)}} = \text{wavenumber (cm}^{-1}\text{)} = \frac{\text{frequency (sec}^{-1}\text{)}}{\text{speed of light (cm sec}^{-1}\text{)}}$$

The fraction of radiant energy that is absorbed depends on the thickness and quality of the medium traversed. The Bouguer-Lambert law of absorption can be stated as:

$$- \frac{dI}{dx} = aI$$

where I is the intensity of light, x a distance into the medium, a the absorption coefficient. Integrating at the boundary conditions ($I = I_0$ when $x = 0$) we have:

$$I = I_0 e^{-ax}$$

In 1852 Beer showed that the coefficient a was proportional to the concentration of the solute C for absorbing compounds in almost transparent solvents. Beer's law is then:

$$I = I_0 e^{-\epsilon cx}$$

where ϵ is the molar extinction coefficient and c the molar concentration.

Spectra of KEtX and C_{12}^{TAB}

All spectra were recorded on a Perkin-Elmer 350 spectrophotometer using Beckman Far UV silica absorption cells for concentrations around $10^{-5} M$ and 1 mm High UV Quartz microcells made by The Ultracell Co. for concentrations in the $10^{-3} M$ range.

Two peaks are present in the UV spectrum of KEtX: one at 301 millimicrons and the other one at 226 millimicrons. A broad band beginning at 219 millimicrons with a deflection point around 194 millimicrons is the only salient characteristic in the spectrum of C_{12}^{TAB} . A molar extinction coefficient could have been calculated say at 200 or 195 millimicrons but in this region oxygen absorption is very strong and special precautions had to be applied not only with respect to the surrounding atmosphere of the instrument (nitrogen purging) but also

with respect to the oxygen content of the sample. For these reasons, as well as because of a moderate contamination background from the apparatus itself appearing below 220 millimicrons, the 301 xanthate peak was considered the most reliable and the least affected one for measuring a change in concentration. The molar extinction coefficient used by Pomianowski and Leja²¹ was 17,750. Majima gives a molar extinction coefficient of 17,460. Because of the change in the high absorbance part of the spectrum, a calibration curve was used to determine the concentrations in every run where the 10^{-3} M solution and the 1 mm cell were used (Fig. 1, Table I). From the graph it can be seen that the extinction coefficient for absorbance units less than 0.7 is constant at 17,500, therefore this value was used to calculate the xanthate concentration for the sphalerite tests in conjunction with the 1 cm cell for concentrations in the 4×10^{-5} M range.

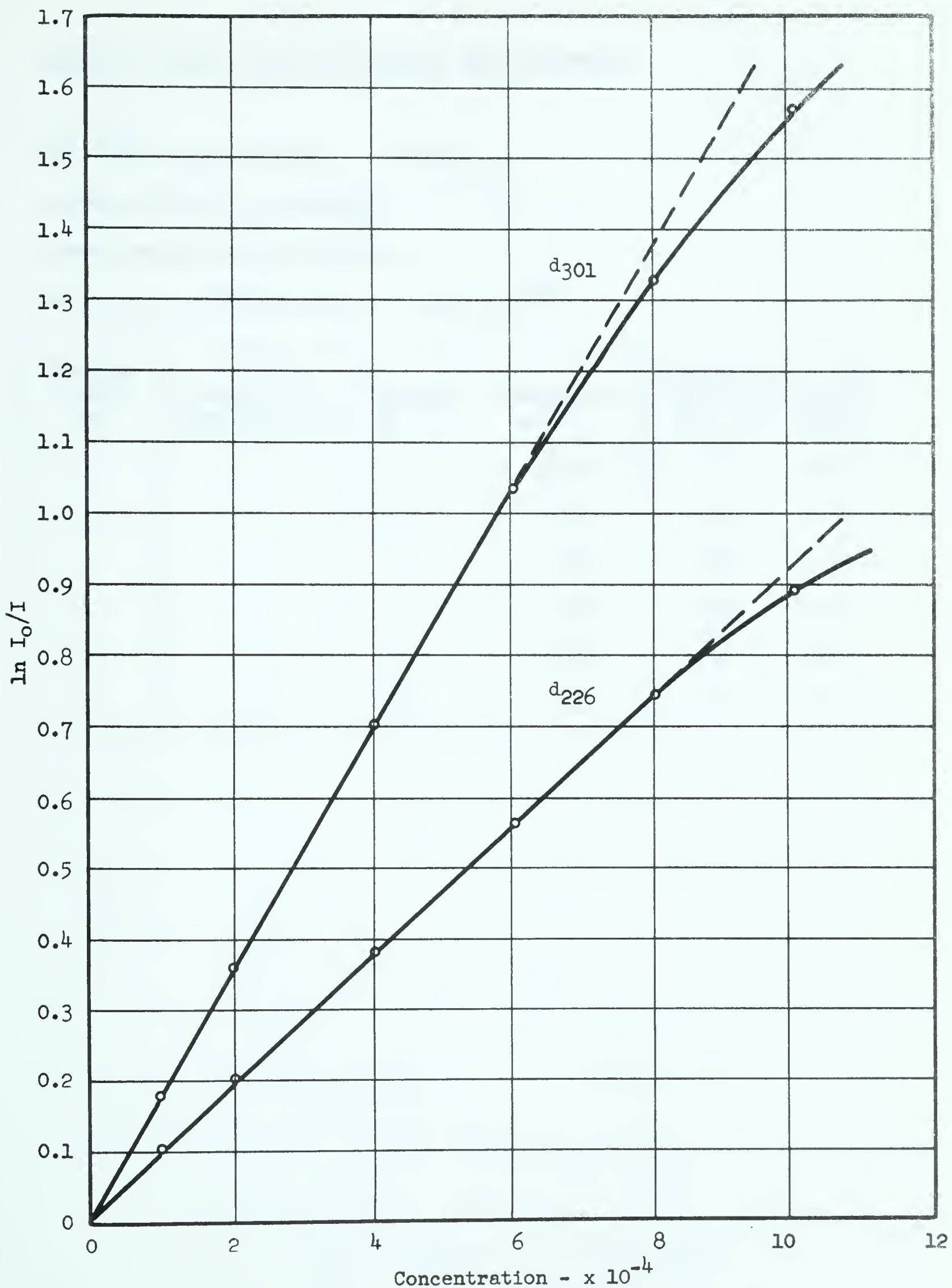


FIG. 1 - BEER'S LAW FOR POTASSIUM ETHYL XANTHATE USING A 1mm QUARTZ CELL.

TABLE I - BEER'S LAW FOR POTASSIUM ETHYL XANTHATE

Molecular weight of KEtX = 160.305 g

 $10^{-3}M$ in 100 ml = 0.01603 g

actual weight used: 0.01621 g

molarity of stock solution = 1.001×10^{-3}

Spectrum Curve No.	1.001x10 ⁻³ M solution - ml	Dilution to ml	Molarity x10 ⁻⁴	Absorbance: $\ln I_0/I$	
				301 m μ	226 m μ
1	10	--	10.01	1.57	0.88
2	8	10	8.01	1.32	0.74
3	6	10	6.01	1.03	0.56
4	4	10	4.00	0.70	0.38
5	2	10	2.00	0.35	0.20
6	1	10	1.00	0.17	0.10

EXPERIMENTAL

Materials

Copper: Reagent grade, electrolytic copper powder (as supplied by Fisher Scientific Co.) was used in all the runs at 10°C. For the second set of runs at 4°C, the size fraction smaller than 38 microns was removed by screening the powder under ether on a 400 mesh Tyler screen. This step was adopted to avoid obstruction of the fritted glass filters in the sample chamber and to avoid the use of excessive pressure at the pump thus reducing the possibility of Tygon tubing failure. The new surface area of the copper powder was measured by adsorption of fatty acids from heptane solution and calculated to be 19,500 cm²/g (Appendix A).

Sphalerite: The powder was prepared from a high purity sample of crystalline sphalerite from Broken Hill, Australia. This material was crushed in a porcelain mortar and pestle and the screened fraction (-65/+ 200 mesh) was washed with distilled water on the 200 mesh screen (74 microns) to remove all of the fines. After a final rinse with doubly distilled water, the sample was dried in a vacuum desiccator.

Chemical analysis indicated the presence of the following elements:

Zn = 66.69%
Fe = 0.17%

Cd = traces
Mn = nil

Pure zinc sulphide consists of 67.09% Zn and 32.91% S.

C_{12}^{TAB}

a) C_{12}^{TAB} used at 10°C was prepared by the late Dr. A. Few in the Department of Colloid Science, Cambridge. Its purity was ascertained by surface tension versus concentration measurements which showed no minimum around the critical micelle concentration.

b) A new sample of C_{12}^{TAB} used in tests at 4°C was supplied by K & K Laboratories Inc. with a guaranteed purity of 95-99%. This sample was subsequently purified by recrystallization from acetone (4 times) extraction with Skellysolve B and final recrystallization from acetone (2 times). Infrared spectrum of this material was identical with the spectrum obtained from the sample described in (a). Unfortunately, no information regarding chainlength can be deduced from the IR spectrum thus rendering impossible any detection of higher and/or lower homologs.

KETX:

Potassium ethyl xanthate was previously prepared in this Department and analyzed 99% in purity. Before starting a series of experiments, the xanthate was washed 6 times with ether to remove any dixanthogen formed on oxidation.

Water:

Low conductivity doubly-distilled water was used throughout the experiments. A value of the specific conductance for a sample taken from one of the storage pyrex bottles was $1.1 \times 10^{-6} \text{ ohms}^{-1} \text{ cm}^{-1}$.

Tygon tubing: A non-toxic clear tubing of plasticized polyvinyl chloride as supplied by Fisher Scientific Co.

Stopcock grease: Dow Corning High Vacuum Grease of the silicone type was selected because it retained its consistency as well as its stability to over 200°C. These conditions were essential because the walls of the sample chamber were heated to 200°C when copper had to be reduced with hydrogen.

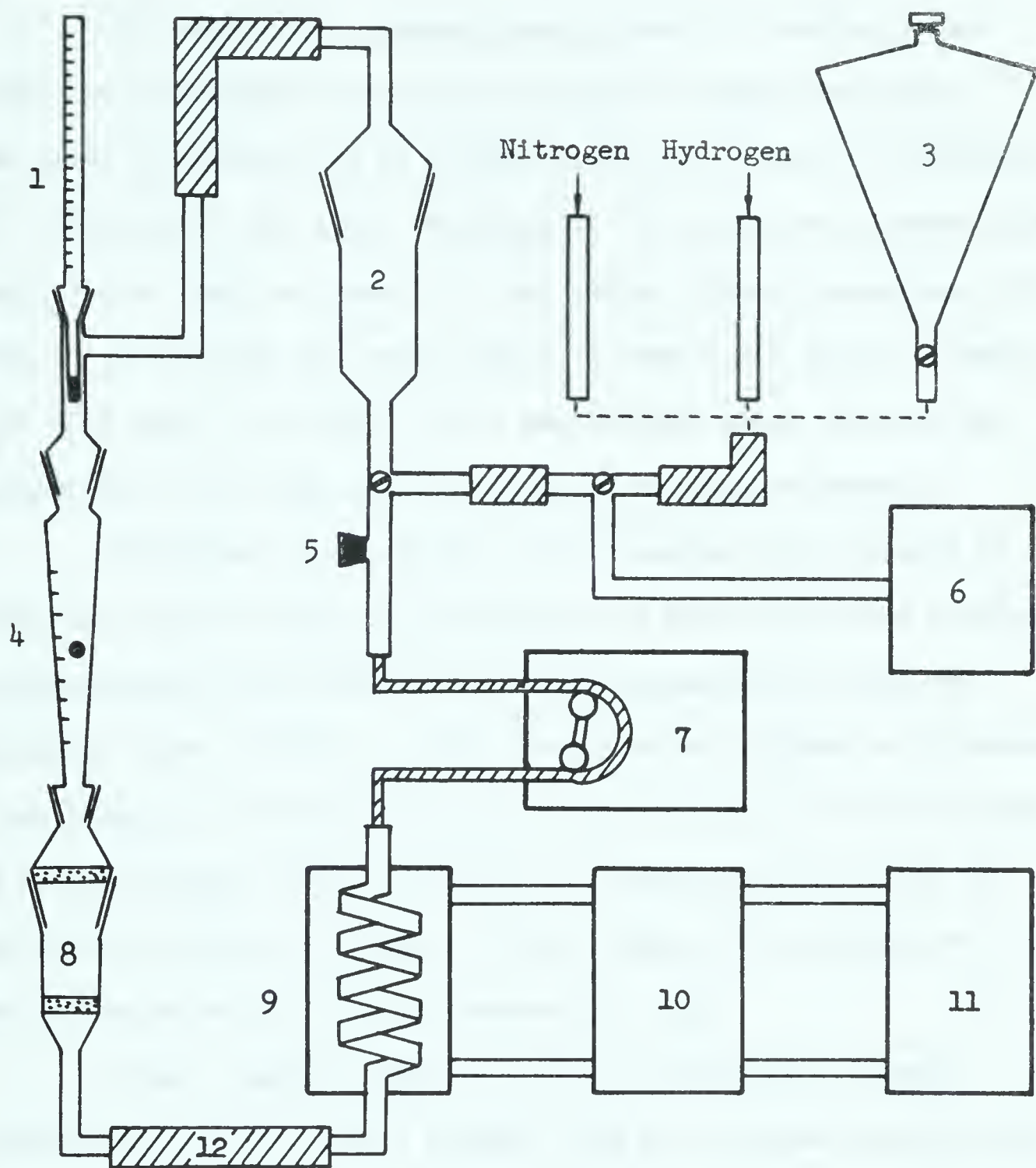
Apparatus:

The apparatus used in these experiments is a modified version of the apparatus used by Pomianowski and Leja²². Some of the innovations include:

- 1) provisions to run tests under a controlled gas atmosphere with all the necessary accessories;
- 2) introduction of a rigid sample chamber with two glass fritted discs of 25-50 microns to facilitate the reduction of copper powder at temperatures above 150°C.
- 3) incorporation of a thermometer with a ground-glass base;
- 4) addition of a refrigerating unit for a more positive control of the temperature.

The arrangement of the adsorption apparatus is shown in Fig. 2.

FIG. 2 - ARRANGEMENT OF THE ADSORPTION APPARATUS



1 Thermometer

2 Receiving vessel

3 Separatory funnel

4 Flow meter

5 Rubber stopper

6 Vacuum pump

7 Circulating pump

8 Sample chamber

9 Cooling coil

10 Controlled temp. bath

11 Refrigerating unit

12 Tygon tubing

Procedure in Systems Open to the Atmosphere

The adsorption apparatus was cleaned by passing a continuous flow of filtered tap water at 40-50°C through the system for at least 30 minutes and by rinsing with three liters of distilled water. The bulk of the water remaining in the system was removed with the peristaltic pump and, later, by injecting filtered compressed air. A Hyvac 14 vacuum pump was used finally to remove all traces of water because this pump is provided with a gas ballast which prevents any contamination of the pump oil when pumping condensable vapours.

Solutions of the surface active agents were prepared by weighing the proper amount of pure agent on a Micro Gram-Atic balance; the concentrations were then checked by UV measurements using the standardized curve in Fig. 1. This procedure was adopted to eliminate the possibility of errors in initial concentrations, in fact the solutions were discarded if the variation in concentration exceeded 5% of the amount measured by weight. In all cases, the solution was cooled in the water bath before commencing a test.

After a proper amount of copper or sphalerite powder was introduced into the sample chamber, 200 ml of cooled solution were added directly to the receiving vessel. Starting of the peristaltic pump was immediately followed by the recording of time beginning at the instant when the solution reached the sample. Running temperature was reached within one minute.

At regular intervals, samples of the circulating solution were temporarily removed for spectrophotometric analysis. After 300 minutes the experiment was stopped, the powder replaced by a fresh

sample and the cycle repeated.

Procedure in Systems under a Nitrogen Atmosphere

Systems under a nitrogen atmosphere were treated basically as above but the following points were modified:

- 1) doubly distilled water was boiled free of oxygen while purified premium nitrogen was bubbled through. (Unpurified premium nitrogen was used only for the series at 10°C);
- 2) solutions of surface active agents were prepared in a dry box and transferred to the system in a well stoppered separatory funnel;
- 3) the apparatus was repeatedly evacuated and filled with purified premium nitrogen through a 3-way stopcock;
- 4) actual transfer of the solution into the system was carried out by a unidirectional flow into the evacuated apparatus with the help of the peristaltic pump; the system was first slightly pressurized by connecting the purified nitrogen line to the 3-way stopcock;
- 5) unavoidable time delays and the design of the apparatus precluded the effective use of a precooled solution. Equilibrium temperature was reached in less than two minutes at 10°C and around three minutes for the runs at 4°C;
- 6) samples removed for spectrophotometric analysis were not returned to the system.

Testing Program and Results

A complete sequence of the tests is given in Table II. After completion of all the runs at 10°C it was realized that more controlled tests were required because of the various combinations chosen, therefore, runs with the amounts of copper other than 10g were omitted from the sequence at 4°C . Extra tests used to plot control curves appear in section (c) of the same table. These tests were required to differentiate runs in an oxygen atmosphere from those runs where oxygen is almost absent. The tests with sphalerite ($4 \times 10^{-5}\text{M}$) were more insensitive to a change in xanthate concentration than the tests with copper powder ($1 \times 10^{-3}\text{M}$) since the formation of a monolayer on the apparatus required a change in concentration of the order of 10^{-6}M . Only few points were available for concentrations of 10^{-3}M whereas a regular pattern appeared where 10^{-5}M solutions were used. This fact suggested a logical way of "filling the gap" in the 10^{-3}M sequence since adsorption mechanism on the apparatus must be the same in both cases. A proof that this correction was far from fictitious is that some of the non-corrected lines have been straightened once this correction has been applied.

The results obtained were graphed as $\log \Gamma$ vs. $\log t$. In all the graphs a definite break appears after a certain time, giving a change in slope: on either side of the break the slope is constant. The first part is referred to as the fast reaction step, the second one as the slow reaction step.

Results have been corrected for every run for adsorption by the apparatus and are presented in graphical form (Figs. 3,

4, 5, 6, 7, 8) in order to avoid incorporation of the original sequence of spectra recorded on the spectrophotometer. A complete analysis and spectra for two of the tests are included in Appendix B.

All of the sphalerite tests have been discarded since the control spectra showed that one cannot differentiate between adsorption on the apparatus and adsorption on the sample. This conclusion is evident from Figs. 9 and 10 (these sphalerite curves overlap regardless of the change in temperature, the only detectable difference being found near the 300 minute value. Here the curve for 4°C shows less adsorption than the one at 10°C).

Adsorption measurements at times longer than 300 minutes have not been attempted because of unavoidable xanthate decomposition, thus altering and impairing the reliability of the measurements. Also, an inevitable mechanical failure of the Tygon tubing at the pump (within 10-15 hours at 10°C and 5 hours at 4°C) discouraged any attempt to prolong adsorption studies.

TABLE II - BASIC TESTING PROGRAM

a) 10°C

		Conditions		Test No.
Sample weight	Solid	Solution	Test No. (KETX)	Test No. (KETX + C_{12}TAB)
1.8g Cu	Not reduced	Aerated	10	11
6.0g Cu	Not reduced	Aerated	12	13
10.0g Cu	Not reduced	Aerated	9 & 46	8 & 47
1.8g Cu	Reduced	Not aerated	27	23
6.0g Cu	Reduced	Not aerated	24	25
10.0g Cu	Reduced	Not aerated	19	18
10.0g Cu	Reduced	Aerated	15	16
10.0g Cu	Not reduced	Not aerated	17	20
50.0g ZnS	--	Aerated	27	28
50.0g ZnS	--	Not aerated	29	30

b) 4°C

Sample weight	Solid	Solution	Test No. (KETX)	Test No. (KETX + C_{12}TAB)
10.0g Cu	Not reduced	Aerated	32	34
10.0g Cu	Reduced	Not aerated	36 C	37
10.0g Cu	Reduced	Aerated	33	35
10.0g Cu	Not reduced	Not aerated	38	39
50.0g ZnS	--	Aerated	40	41
50.0g ZnS	--	Not aerated	42	43 & 44

c) Control tests

Adsorption on apparatus and decomposition of mixture	Temp.	Solution	Path length of cell	Test No.
	10°C	Not aerated	1 cm	50
	10°C	Not aerated	1 mm	48
	4°C	Aerated	1 cm	45
	4°C	Not aerated	1 cm	49

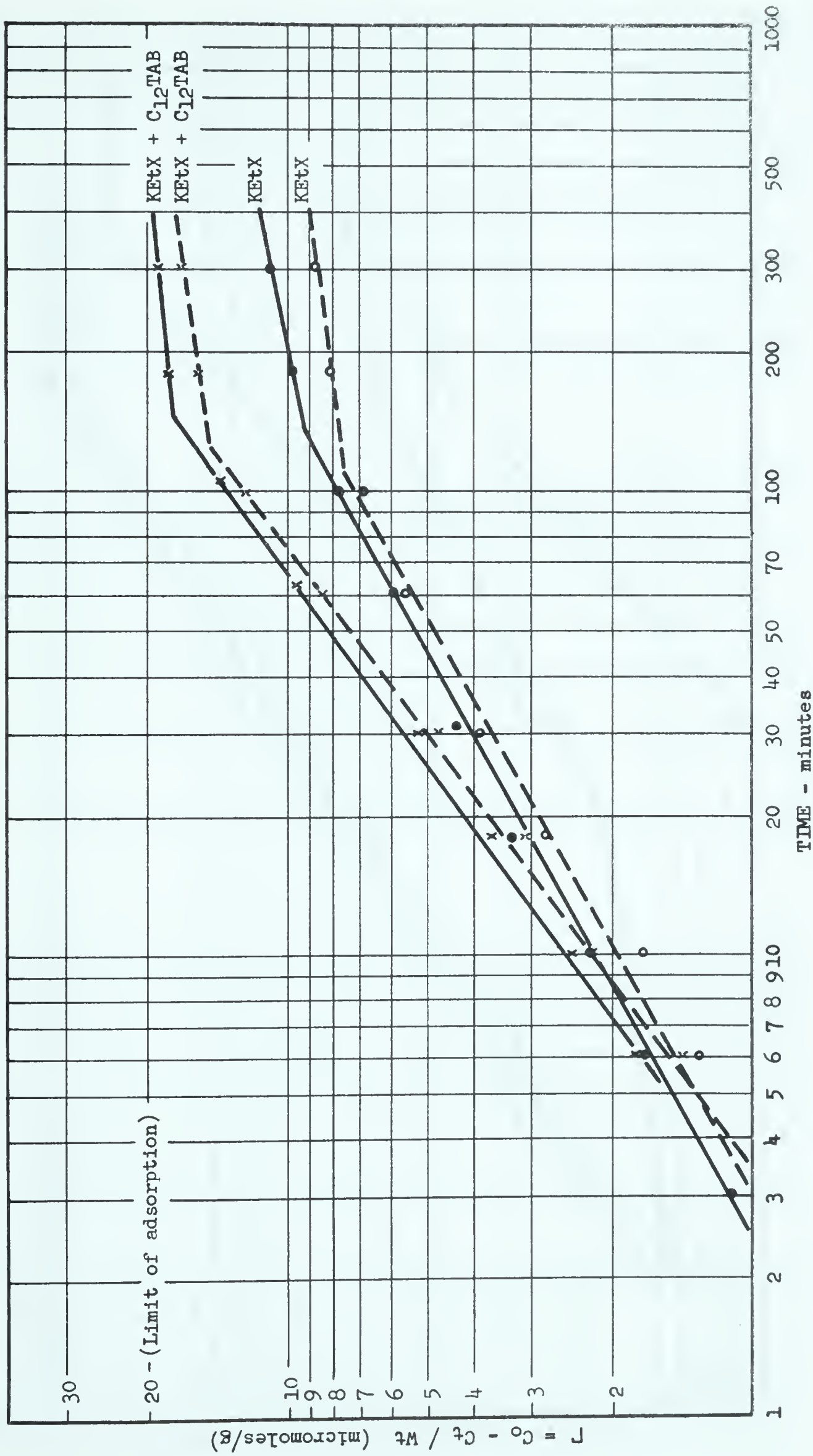


FIG. 3 - ADSORPTION OF KETX AND MIXTURE OF KETX AND C₁₂TAB ON 10g OF COPPER (NOT REDUCED) IN SYSTEMS OPEN (-) AND CLOSED (--) TO THE ATMOSPHERE AT 10° C.

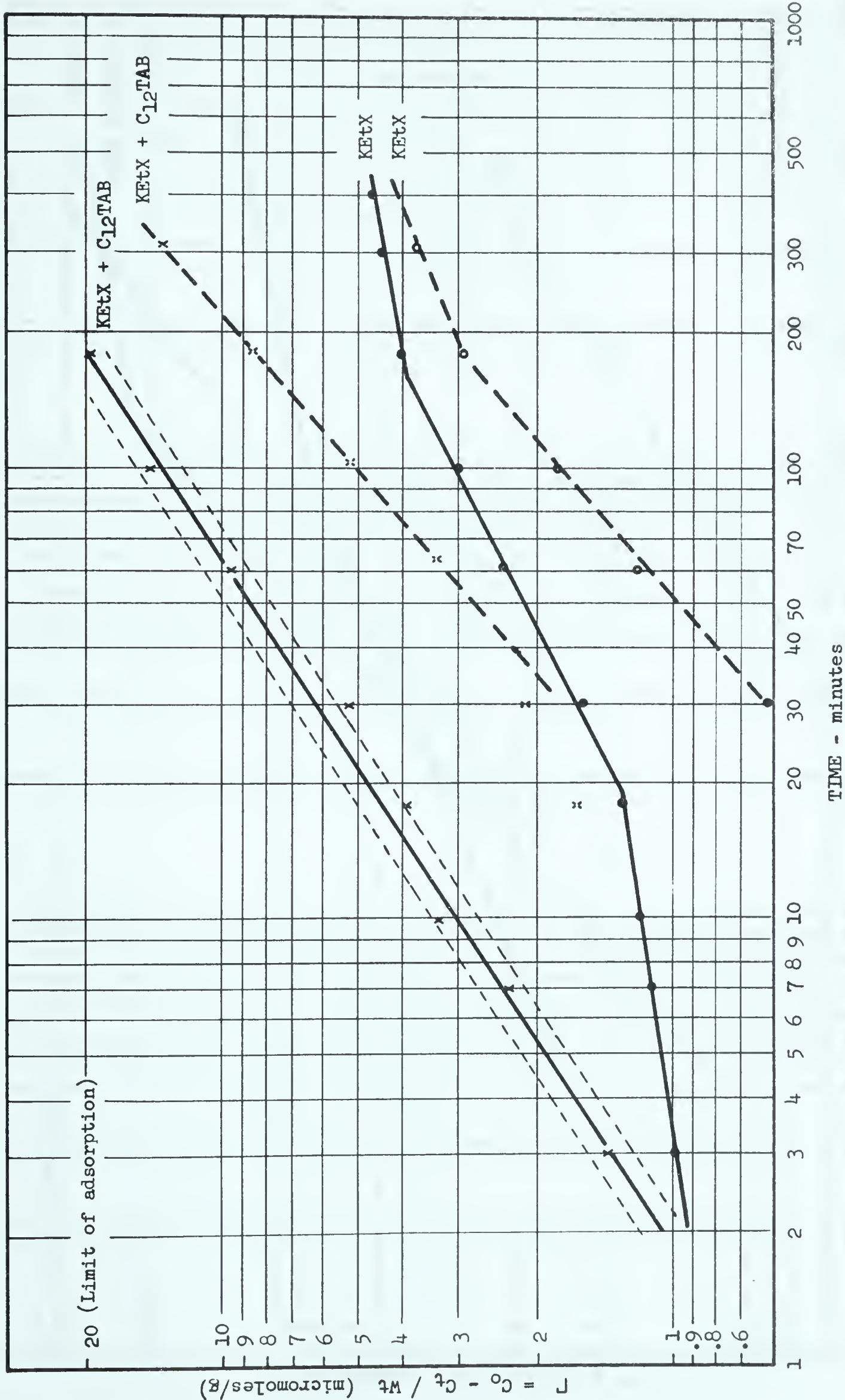


FIG. 4 - ADSORPTION OF KETX AND MIXTURE OF KETX AND C₁₂TAB ON LOG OF COPPER (REDUCED) IN SYSTEMS OPEN (-) AND CLOSED (--) TO THE ATMOSPHERE AT 10° C.

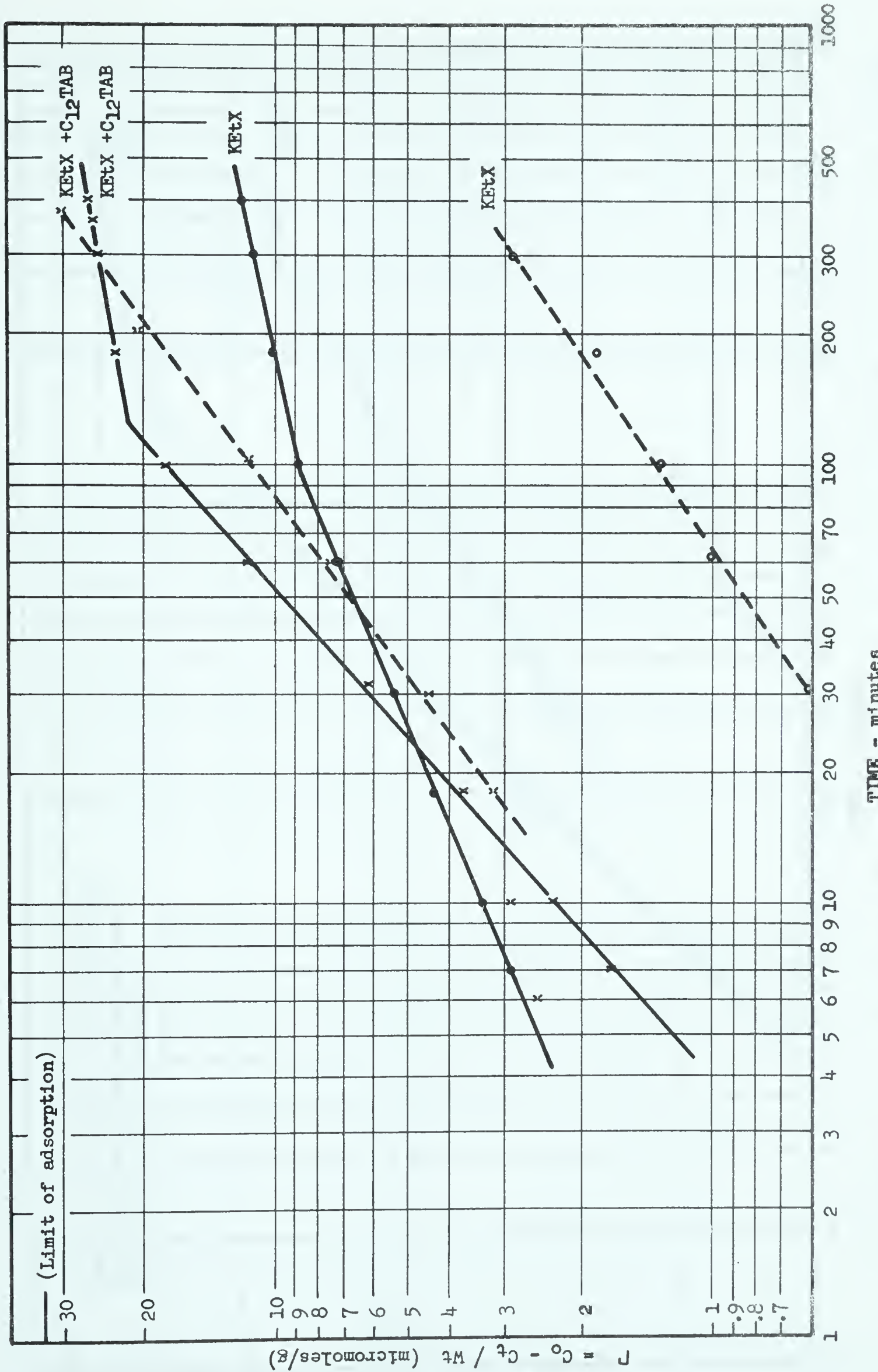


FIG. 5 - ADSORPTION OF KETX AND MIXTURE OF KETX AND C₁₂TAB ON 6g OF COPPER (REDUCED: -- and NOT REDUCED: -) IN A SYSTEM OPEN TO THE ATMOSPHERE AT 10° C.

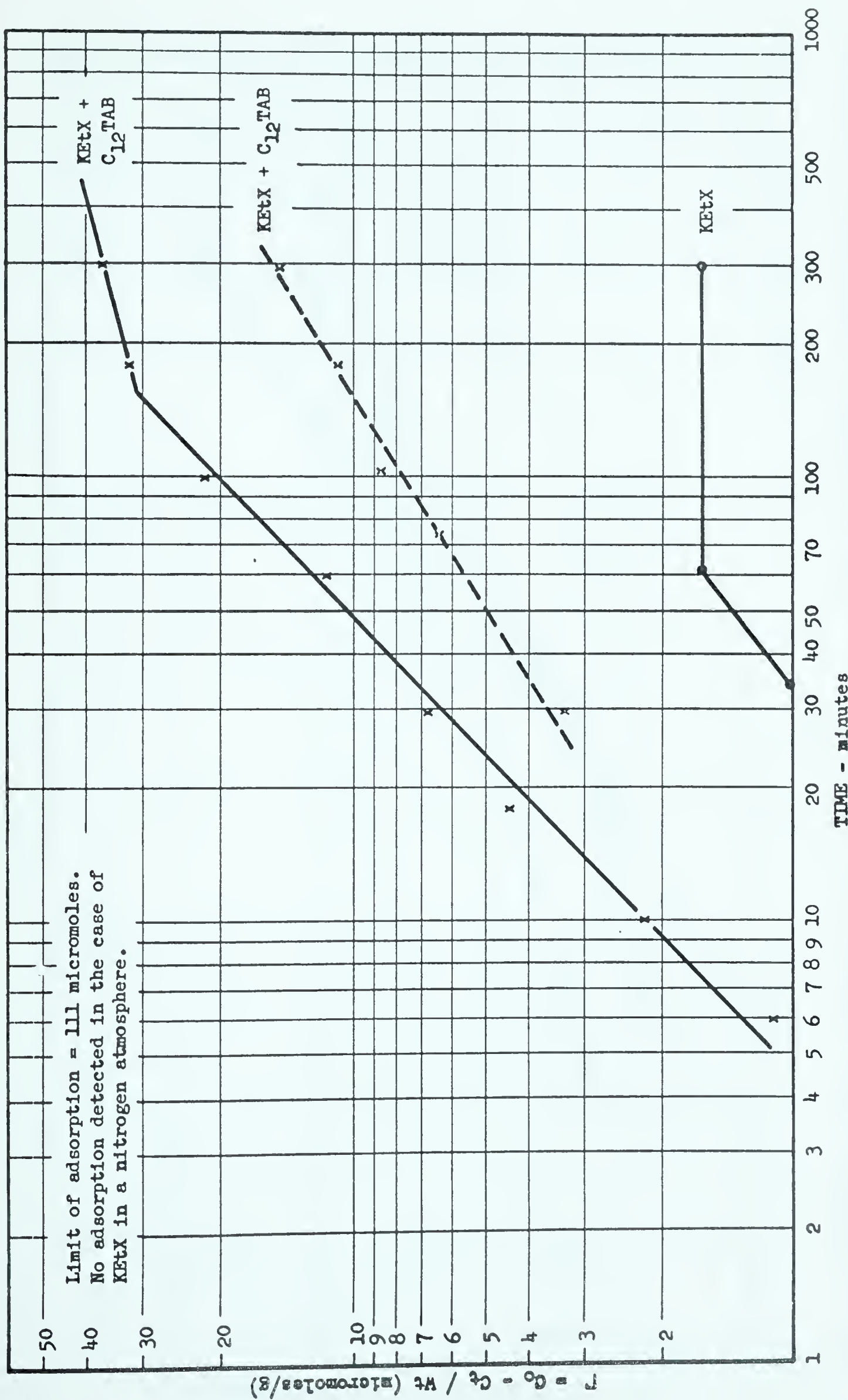


FIG. 6 - ADSORPTION OF KETX AND MIXTURE OF KETX AND C₁₂TAB ON 1.8g OF COPPER (REDUCED: -- and NOT REDUCED: -) IN SYSTEMS OPEN (-) AND CLOSED (--) TO THE ATMOSPHERE AT 100 C.

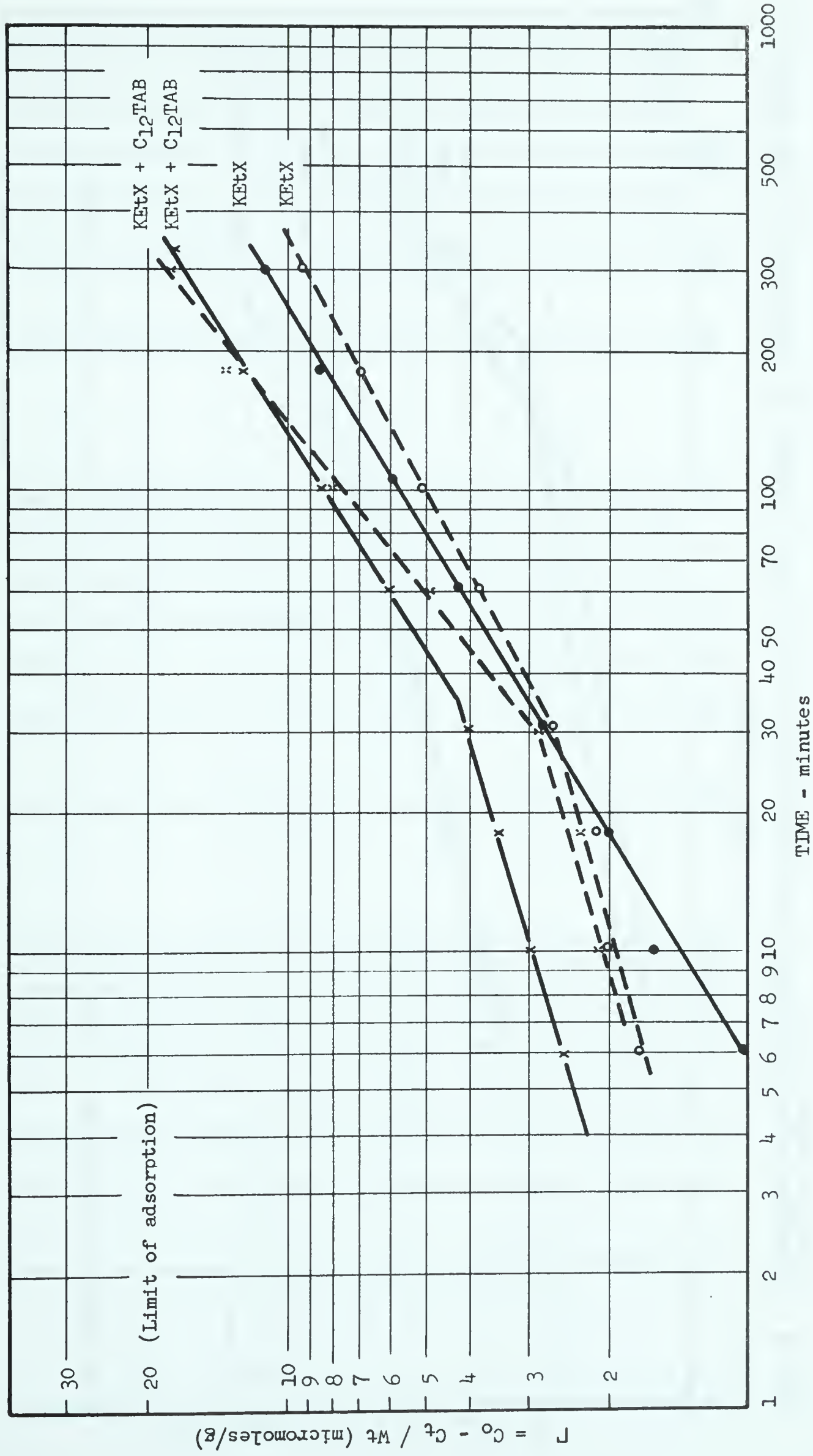


FIG. 7 - ADSORPTION OF KETX AND MIXTURE OF KETX AND C₁₂TAB ON 10g OF COPPER (NOT REDUCED) IN SYSTEMS OPEN (—) AND CLOSED (---) TO THE ATMOSPHERE AT 40° C.

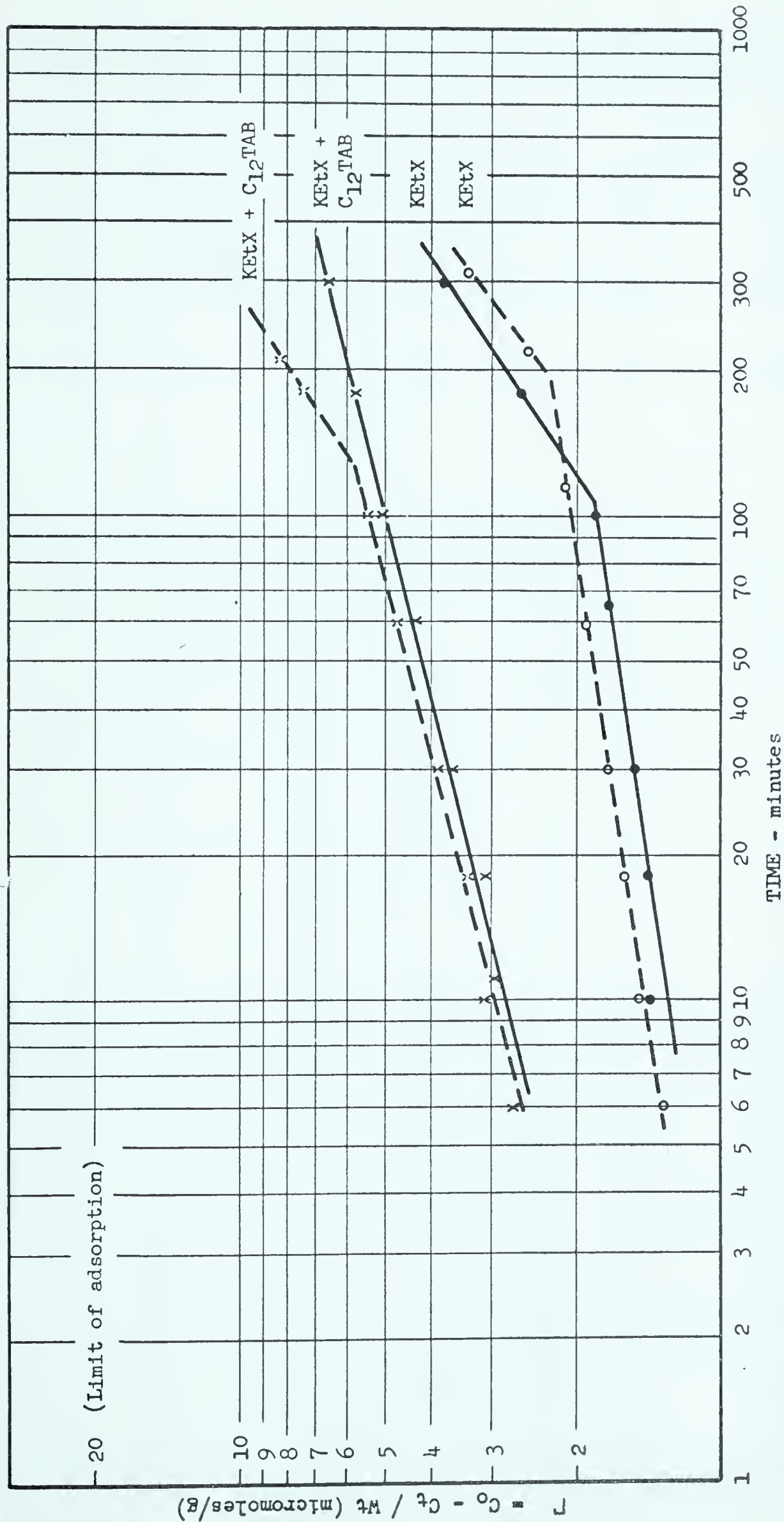


FIG. 8 - ADSORPTION OF KETx AND MIXTURE OF KETx AND C₁₂TAB ON 10g OF COPPER (REDUCED) IN SYSTEMS OPEN (-) AND CLOSED (--) TO THE ATMOSPHERE AT 40°C.

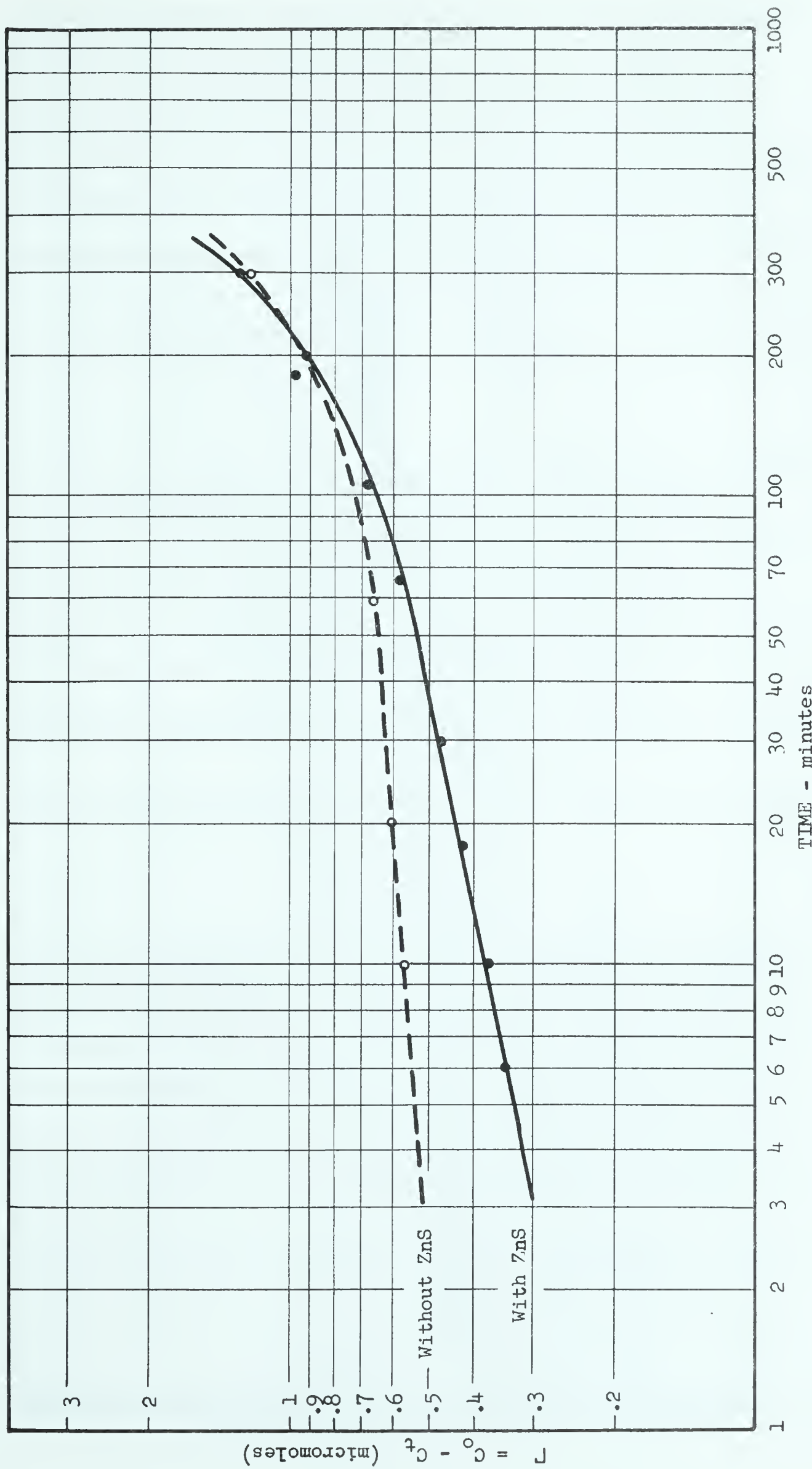


FIG. 9 - ADSORPTION ON THE APPARATUS AND DECOMPOSITION OF KETx AND C₁₂TAB IN TESTS WITH AND WITHOUT SPHALERITE AT 10° C IN A NITROGEN ATMOSPHERE.

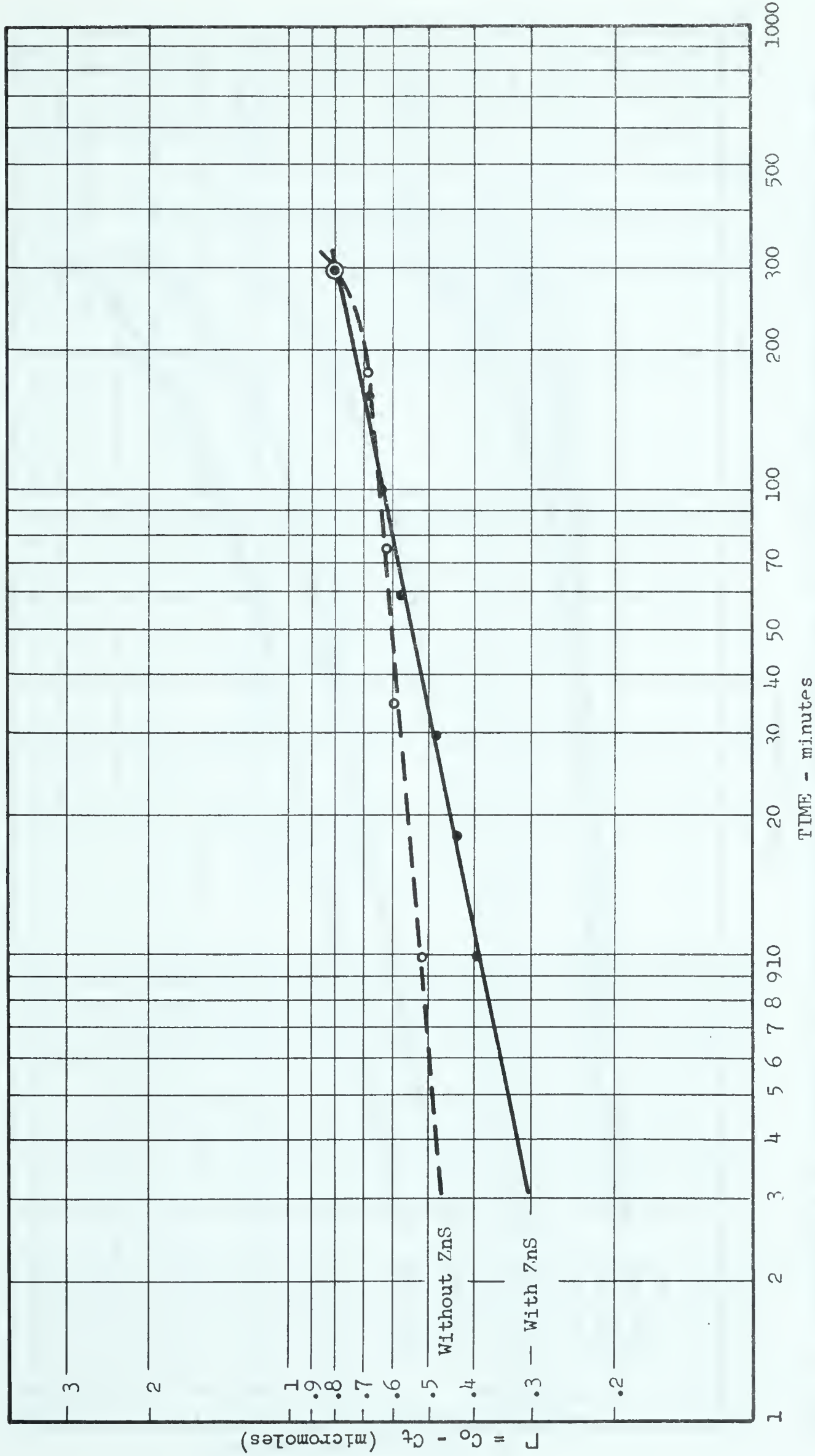


FIG. 10 - ADSORPTION ON THE APPARATUS AND DECOMPOSITION OF KETX AND $C_{12}TAB$ IN TESTS WITH AND WITHOUT SPHALERITE AT $40^{\circ}C$ IN A NITROGEN ATMOSPHERE.

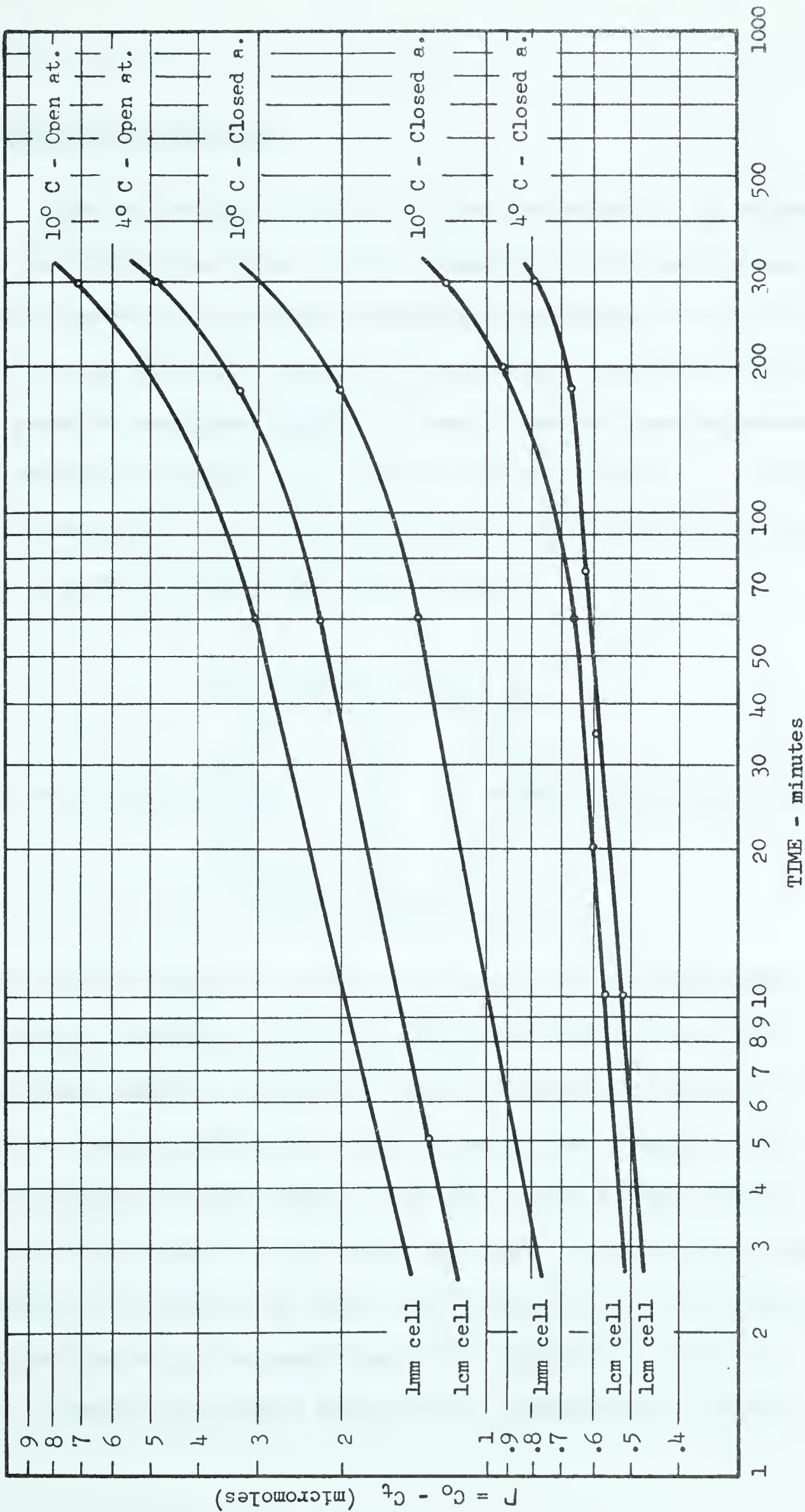
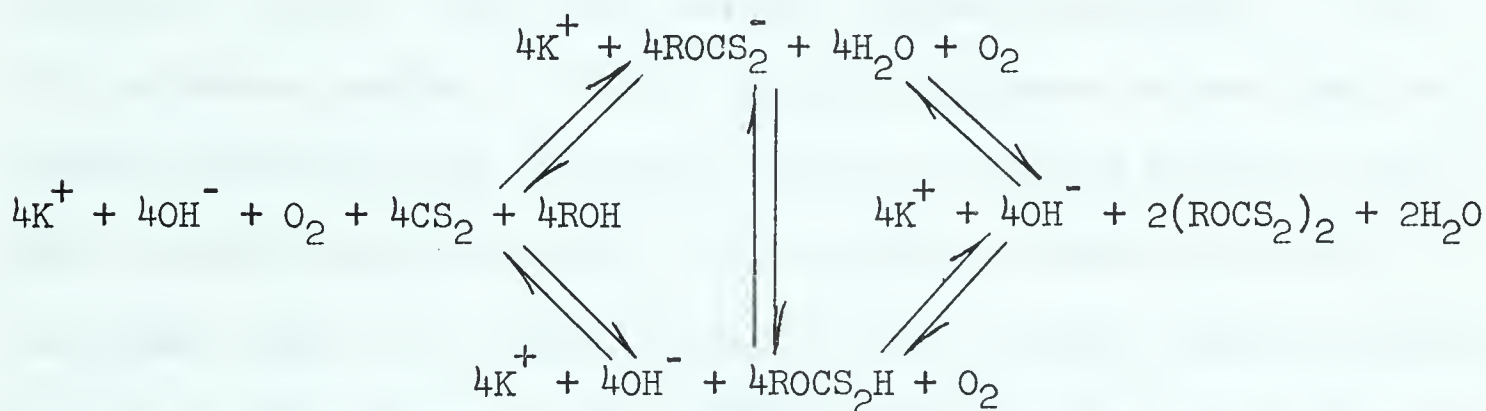


FIG. 11 - ADSORPTION ON APPARATUS AND DECOMPOSITION OF KETX AND C₁₂TAB AT DIFFERENT TEMPERATURES IN SYSTEMS OPEN AND CLOSED TO THE ATMOSPHERE.

DISCUSSION

Stoichiometry of the Reaction

The most complete account for the stoichiometry of xanthate reactions in solution has been recently suggested by Pomianowski and Leja²¹. These authors review the relevant literature concerning the dissociation, decomposition and stability constants of many alkyl xanthates as well as the most probable reactions involved. From a detailed spectrophotometric study of xanthate solutions they conclude that the following six reactions must be accounted for in a complete description of the presence of various species at a given pH, temperature and pressure:



All kinetic studies require a proper assessment of the stoichiometry of the reactions, especially if other complexing agents are present (e.g. quaternary ammonium compounds), but the inherent complexity of the reactions renders difficult a detailed analytical account of all the species present in each sample. For this reason a fast physical means of detection like UV spectroscopy was used. Since only two maxima are exhibited by a solution of KETX, and the peak at 301 millimicrons was least influenced by the adsorption on the apparatus, presence of available inorganic and organic gegen ions, it seemed most logical to

follow the changes in xanthate concentration by the maximum at 301 millimicrons.

A "molecular association" has been described by Buckenham and Schulman²³ in the form of a 1:1 complex between a xanthate anion and a C_{12} TAB cation. Following the work of Bowcott²⁴ on the penetration of long chain amine monolayers by soluble xanthate molecules and the consequent stabilization against atmospheric oxidation of the latter at the air/water interface, Buckenham and Schulman showed that a strong association takes place at the air/water interface when xanthates and quaternary ammonium compounds are combined. Their study of changes in surface tension measurements vs. various molar ratios indicated that the xanthates and the substituted ammonium compounds associate to form a 1:1 molecular complex. It is of primary importance to note that the stabilized mixed films obtained by Bowcott collapsed whenever iodine was injected beneath the film. This transient stabilization will be discussed later on in terms of relative bond strength between xanthates species in dixanthogen, metal xanthates and molecular associations in solutions.

Studies of Mixtures of Xanthates and C_n TAB

It has been pointed out by Pomianowski and Leja²² that equimolar mixtures of KC_9X and C_{12} TAB on mixing immediately formed a precipitate. Homologs of higher chain length also produced a precipitate on mixing while a combination of KC_6X and C_{12} TAB did not produce a precipitate even after standing for a month in a stoppered volumetric flask (an imperceptible opalescence appeared after a few days

similar to the one displayed by solutions of xanthates alone). Whenever precipitates were obtained these were filtered, dried in a vacuum desiccator, chemically analized and their x-ray diffraction patterns compared with those of the original components.

a) Chemical Composition

Microchemical analyses (performed by Dr. F. Pascher of Bonn, Germany) are presented in Tables III and IV. No bromine was detected in any of the precipitates. The results indicate that the most likely chemical composition is the 1:1 ratio of the individual species and that the oxygen assay is the most difficult to reproduce since the precipitates are hygroscopic to various degrees. A further discrepancy between the chemical assay and the calculated molecular association can be partially explained if we consider the possibility of higher and/or lower chain homologs in the C₁₈TAB used (even though no minimum is reported for this compound around the critical micelle concentration in surface tension vs. concentration measurements).

b) X-ray diffraction

X-ray powder diffractions techniques have been used successfully by Warren and Matthews²⁵ to identify alcohols by their xanthates derivatives and by Brock and Hannum²⁶ for the identification of amines. X-ray diffraction patterns of the individual xanthates and amines used in these experiments were recorded and their spacings compared with those obtained in patterns of the precipitates (Table V). In no case the d-spacings of these precipitates agreed with d-spacings of the constituents thus suggesting that a new compound or a complex was formed (Fig. 12).

TABLE III - PERCENTAGE COMPOSITION OF KC_6X , $C_{18}TAB$ (CALCULATED FROM EXACT FORMULA) AND THE CORRESPONDING PRECIPITATE FROM AN EQUIMOLAR MIXTURE OF THE TWO (ACTUAL ASSAY AND CALCULATED 1:1 RATIO).

ELEMENT	KC_6X (A)	$C_{18}TAB$ (B)	PRECIPITATE		
			ACTUAL ASSAY WITH WATER	ACTUAL ASSAY WITHOUT WATER	CALCULATED (A):(B) RATIO
C	38.9	64.3	65.28	68.2	68.7
H	6.0	11.7	10.58	11.0	12.1
N	-	3.6	2.33	2.4	2.8
O	7.4	-	5.75	6.0	3.3
S	29.6	-	11.82	12.4	13.1
K	18.1	-	-	-	-
Br	-	20.4	-	-	-
Sub total	-	-	95.76	-	-
H_2O	-	-	4.83	-	-
TOTAL	100.0	100.0	100.59	100.0	100.0

TABLE IV - PERCENTAGE COMPOSITION OF KC_9X , $C_{12}TAB$ (CALCULATED FROM EXACT FORMULA) AND THE CORRESPONDING PRECIPITATE FROM AN EQUIMOLAR MIXTURE OF THE TWO (ACTUAL ASSAY AND CALCULATED 1:1 RATIO).

ELEMENT	KC_9X (A)	$C_{12}TAB$ (B)	PRECIPITATE		
			ACTUAL ASSAY WITH WATER	ACTUAL ASSAY WITHOUT WATER	CALCULATED (A):(B) RATIO
C	46.4	58.5	64.67	69.0	67.1
H	7.4	11.1	10.25	10.9	11.9
N	-	4.5	1.96	2.1	3.1
O	6.2	-	4.28	4.6	3.6
S	24.8	-	12.56	13.4	14.3
K	15.2	-	-	-	-
Br	-	25.9	-	-	-
Sub total	-	-	93.72	-	-
H_2O	-	-	5.92	-	-
TOTAL	100.0	100.0	99.64	100.0	100.0

TABLE V - X-RAY DIFFRACTION DATA.

KC ₆ X		KC ₉ X		C ₁₂ ^{TAB}		C ₁₈ ^{TAB}	
d	I/I ₀	d	I/I ₀	d	I/I ₀	d	I/I ₀
13.8	1.00	17.8	1.00	21.8	1.00	28.0	1.00
6.9	.08	8.91	.20	10.9	.44	14.0	.74
4.62	.07	5.93	.19	5.76	.36	9.40	.22
4.51	.06	4.72	.01	4.34	.55	5.64	.28
4.25	.01	4.53	.01	4.21	.08	4.70	.50
4.00	.05	4.46	.01	3.61	.29	4.13	.15
3.26	.01	4.43	.02	3.37	.02	4.03	.38
3.09	.03	4.22	.01	3.09	.07	3.63	.09
3.02	.02	3.56	.05	2.54	.01	3.53	.26
2.92	.04	3.14	.01	2.46	.03	3.14	.09
		2.97	.03	2.28	.02	2.35	.08
		2.88	.01	2.08	.02		
		2.55	.02				
		2.28	.01				

KC ₆ X + C ₁₈ ^{TAB}		KC ₉ X + C ₁₂ ^{TAB}		KC ₉ X + C ₁₈ ^{TAB}	
d	I/I ₀	d	I/I ₀	d	I/I ₀
44 ± 5	1.00	42 ± 5	1.00	32.7	1.00
17.5	.02	26.1	.20	11.0	.03
10.1	.01	14.2	.01	8.26	.05
7.5	.01	7.07	.01	6.60	.15
6.08	.02	6.70	.03	5.30	.03
5.30	.01	5.40	.01	4.83	.03
4.75	.04	4.98	.01	4.73	.05
4.36	.03	4.48	.03	4.38	.21
4.27	.03	4.33	.01	3.85	.12
3.83	.06	4.09	.04	3.69	.03
3.66	.03	4.02	.02	3.30	.04
3.50	.01	3.85	.01		
3.04	.01	3.45	.01		
2.78	.01	3.16	.01		
2.49	.01				
2.11	.01				

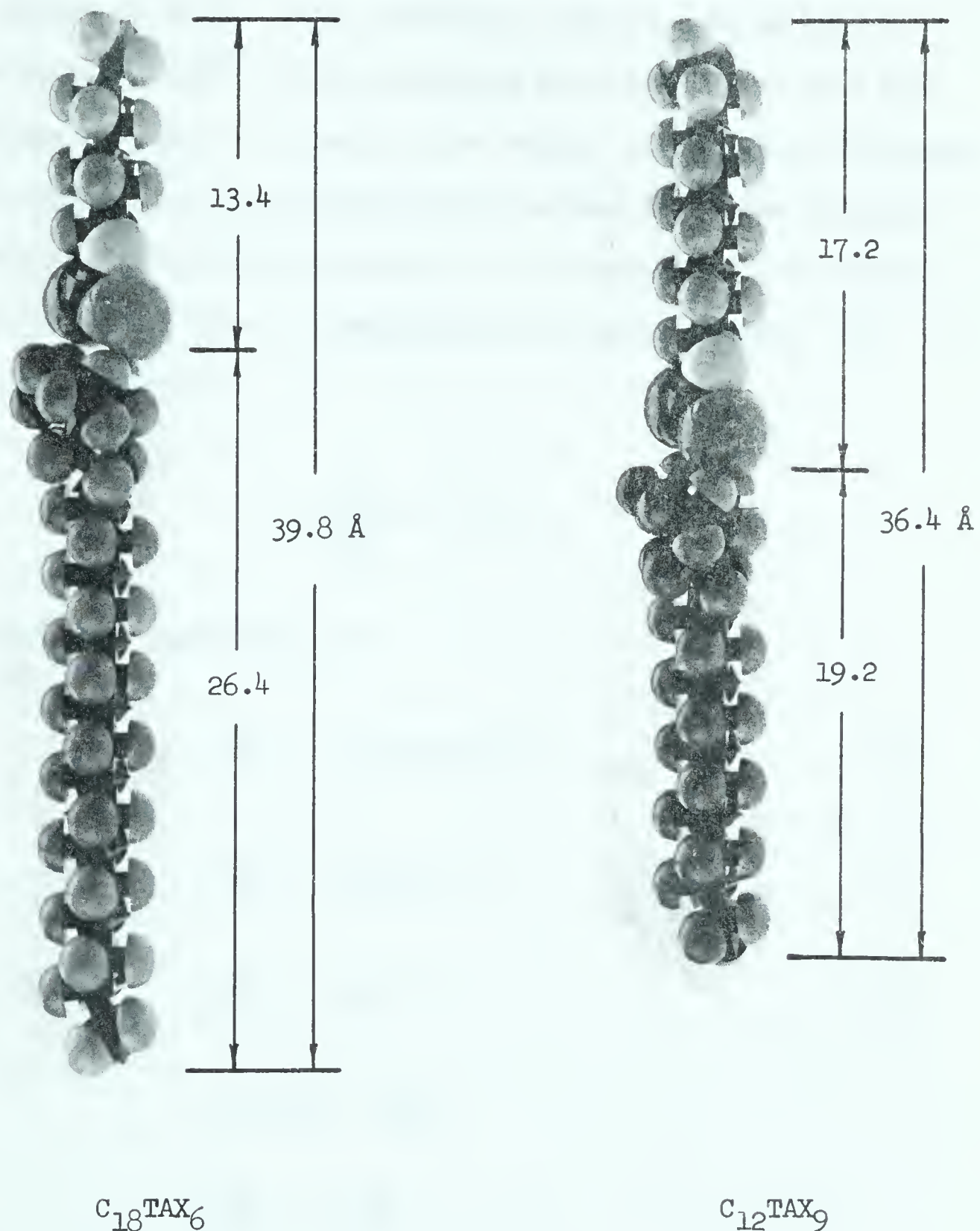
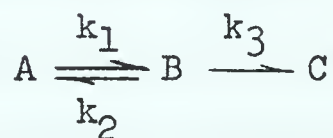


FIG. 12 - PROPOSED HEAD-TO-HEAD ARRANGEMENT OF THE PRECIPITATES FORMED FROM EQUIMOLAR SOLUTIONS OF C_{18}TAB WITH KC_6X AND C_{12}TAB WITH KC_9X .

Role of Intermediates in Organic Reactions

Many reactions that appear simple in reality take place through a series of steps. Such a mechanism implies a formation of a reactive intermediate²⁷. An intermediate has been defined as a temporary minimum in a plot of standard free energy vs. reaction coordinate. A proper description of any mechanism must account for these intermediates as well as for transition states which correspond to the maxima in the plot described above. Intermediates can be classified. If we consider the reaction:



by the steady state approximation:

$$\frac{dB}{dt} = k_1 A - k_2 B - k_3 B = 0 \quad (1)$$

$$\frac{dA}{dt} = k_2 B - k_1 A = 0 \quad (2)$$

$$\frac{dC}{dt} = k_3 B = 0 \quad (3)$$

from (1): $k_2 B - k_1 A = -k_3 B$

or: $\frac{dA}{dt} = -\frac{dc}{dt}$

again from (1): $k_1 A = k_2 B + k_3 B$

$$k_1 A = (k_2 + k_3) B$$

$$B = \frac{k_1}{k_2 + k_3} A$$

therefore from (3):

$$\frac{dc}{dt} = k_3 B = \frac{k_1 k_3}{k_2 + k_3} A = \frac{k_1}{k_2/k_3 + 1} A$$

Now if $k_2 \approx k_3$ the total rate is affected by the rate of bonding (k_1) and by the rate of partitioning ($k_2/k_3 \approx 1$ and $\frac{dc}{dt} \approx \frac{k_1}{2} A$), the intermediate is called van't Hoff intermediate. If $k_2 \gg k_3$ a pre-equilibrium occurs and an Arrhenius type of intermediate is formed. If $k_3 \gg k_2$, k_1 is the rate-determining step of the reaction.

Chemical structure can also be used to classify intermediates. In our system we should differentiate between these real intermediates and the possible "chemical compound or complex" formed when xanthate anions unite with $C_n TAB$ cations. The evidence for the existence of these compounds is presented under the heading: "Studies of Mixtures of Xanthates and $C_n TAB$ ". Further studies on the properties of these compounds are presently carried on in this laboratory.

It would be of interest to find the equilibrium constants for each of these precipitates (e.g. by conductivity measurements) and to compare their values to the solubility products of each constituent as found in the literature. The result of investigations such as this could add validity to the already strong opinion that the reacting species is a weakly bonded compound formed through a reorganization of the molecular structure.

Sowden and Davidson²⁸ produced free radicals by photolysis and isolated them in a solid matrix at low temperature. In recent

years, it has been possible to detect a reaction intermediate with the aid of sensitive spectrophotometers. These intermediates are easily detected by the appearance or disappearance of an adsorption band at a characteristic wavelength. It is most unfortunate that a thermostatically-controlled flow cell was not used in the present work rendering impossible any detection of an intermediate which might have formed during adsorption since equilibrium conditions were most certainly obtained in handling the sample out of the system. A special kind of intermediate, a charge transfer complex involving acceptor and donor molecules, has been investigated by Mulliken²⁹. From a general definition of donors (D) and acceptors (A) as "those entities such that, during the interaction between (D) and (A), a transfer of negative charge from (D) to (A) takes place, with the formation as end-products either of additive combinations or new entities", Mulliken gives the wave function ψ of the stable or transitory 1:1 complex (AD) as:

$$\psi \approx a\psi_0(AD) + b\psi_1(A^-D^+) \quad (1)$$

This equation describes a partial transfer of an electron from (D) to (A) but does not necessarily imply a sharing of an electron pair or a complete transfer of an electron from atom (D) to (A). "Without an explicit quantum mechanical formulation, the nature of partial electron transfer has tended to appear rather obscure"²⁹. Moreover: "The structure of any loose 1:1 molecular complex or compound between neutral closed-shell entities can be described as:

$$\psi_N = a\psi_0(D,A) + b\psi_1(D^+ - A^-)$$

where $\psi_0(D, A)$ represents a no-bond structure and $\psi_1(D^+ - A^-)$ a dative structure". An intermolecular charge transfer spectrum must exist if an excited state E is formed. Intense spectra due to charge transfers are then possible even for very loose complexes and have been obtained for a number of complexes by various authors named in the paper.

Complete description of a reaction path and mechanism is restricted by a quantum-mechanical symmetry requirement inherent but beyond the scope of the present work.

Of the remaining methods of detecting intermediates (e.g. entropies of activation, radioactive tracers etc.), the reaction order is one of the easiest to apply to the data obtained in this study and is fully discussed in the next section.

Reaction Order

It is common knowledge that the kinetic order of a reaction can imply the presence of an intermediate especially if the order of the reaction differs from the stoichiometry. To explain this apparent inconsistency the postulate of reaction intermediate has been extensively used. Ingold³⁰ provided an explanation of the principle using the following analogy: "If two horses nibble the same haystack, neither interferes with the meal of the other because there is plenty of haystack; but if the two are jointly hand-fed, one straw at the time (from a limited source), then what one gets the other must go without. In the first case the feedings are additive; in the second they are complementary. That is the whole principle".

In an attempt to establish the reaction order by graphical methods, the following quantities have been plotted versus time (Fig. 13):

- a) $(C_o - C_t)$ for a zero order reaction
- b) $\ln(C_o - C_t)$ for a first order reaction
- c) $\frac{1}{\ln(C_o - C_t)}$ for a second order reaction
- d) $\frac{1}{\ln(C_o - C_t)^2}$ for a third order reaction

In all cases the lines gradually changed slope thus rendering difficult if not impossible a proper determination of the reaction order and the rate constant. It should be noted that all of the points pertaining to both fast and slow steps of the reaction appear on the graph and that the plot corresponding to the second order reaction consists of two straight lines (Fig. 13).

The half life method is a successful alternative for an evaluation of the reaction order. In a general case we have:

$$-\frac{dc}{dt} = kC^n$$

$$\int -\frac{dc}{C^n} = \int kdt$$

$$-\left[\frac{1}{(n-1)(C^{n-1})} \right] \begin{matrix} C \\ c/2 \end{matrix} = k\tau$$

$$-\frac{1}{(n-1)(C^{n-1})} + \frac{2^{n-1}}{(n-1)(C^{n-1})} = k\tau$$

$$\tau = \frac{2^{n-1} - 1}{k(n-1)(C^{n-1})}$$

Where C is the initial concentration, n the reaction order and τ the half life. If we know two different initial concentrations, C_1 and

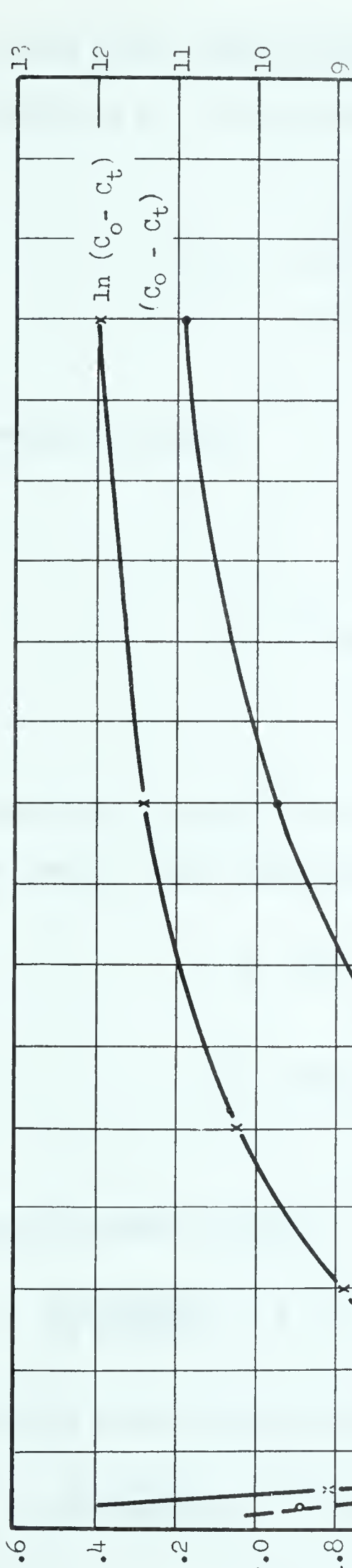
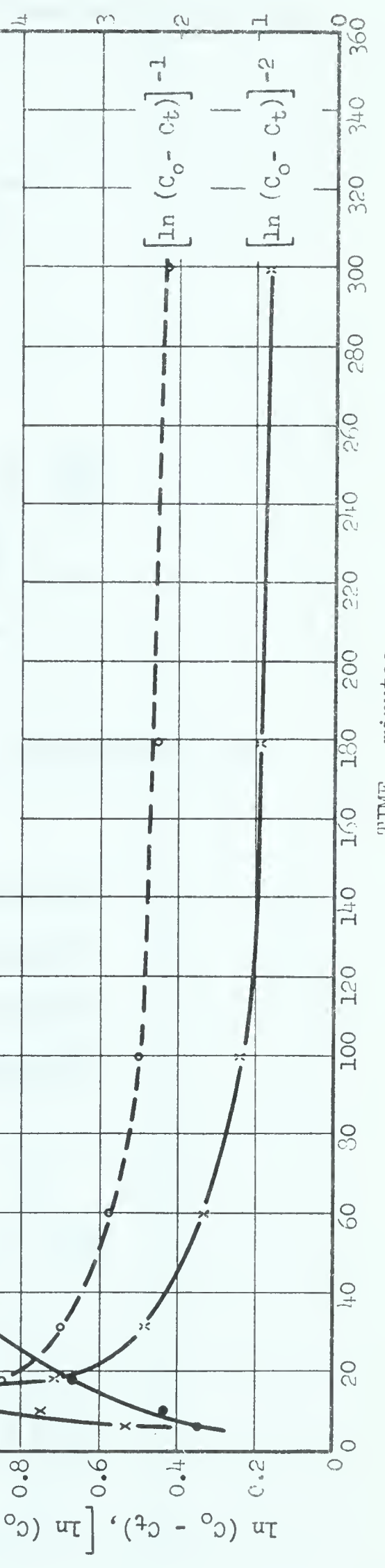


FIG. 13 - GRAPHICAL REPRESENTATION OF ZERO, FIRST, SECOND AND THIRD ORDER REACTIONS FOR KETX IN A TEST ON COPPER POWDER AT 100°C IN A SYSTEM OPEN TO THE ATMOSPHERE.

$$L = C_0 - C_t \text{ (microMoles/g)}$$



$$\ln (C_0 - C_t), [\ln (C_0 - C_t)]^{-1}, [\ln (C_0 - C_t)]^{-2}$$

TIME - minutes

C_2 , and their respective half lives, τ_1 , and τ_2 , we can easily calculate the order, n , of the reaction:

$$\frac{\tau_1}{\tau_2} = \frac{\frac{2^{n-1} - 1}{(n-1)(C_1^{n-1})k}}{\frac{2^{n-1} - 1}{(n-1)(C_2^{n-1})k}} = \left[\frac{C_2}{C_1} \right]^{n-1}$$

Taking logarithms:

$$\ln \frac{\tau_1}{\tau_2} = (n-1) \ln \frac{C_2}{C_1}$$

$$n = \text{reaction order} = \frac{\ln \frac{\tau_1}{\tau_2}}{\ln \frac{C_2}{C_1}} + 1$$

From Figs. 14 and 15 the projected half lives and concentrations for the range of fast abstraction of xanthate are:

$$\begin{aligned} \text{a) KETX:} \quad &= 165 \text{ min } C_2 = 0.99 \times 10^{-3} \text{ M} \\ &= 315 \text{ min } C_1 = 0.49 \times 10^{-3} \text{ M} \\ \text{b) Mixture:} \quad &= 92 \text{ min } C_2 = 1.00 \times 10^{-3} \text{ M} \\ &= 200 \text{ min } C_1 = 0.50 \times 10^{-3} \text{ M} \end{aligned}$$

Reaction order for KETX:

$$n = \frac{\ln 315/165}{\ln 0.99/0.49} + 1 = \frac{\ln 1.91}{\ln 2.02} + 1 = \frac{0.645}{0.704} + 1 = 1.92$$

Reaction order for the mixture:

$$n = \frac{\ln 200/92}{\ln 1.00/0.50} + 1 = \frac{\ln 2.17}{\ln 2} + 1 = \frac{0.775}{0.693} + 1 = 2.12$$

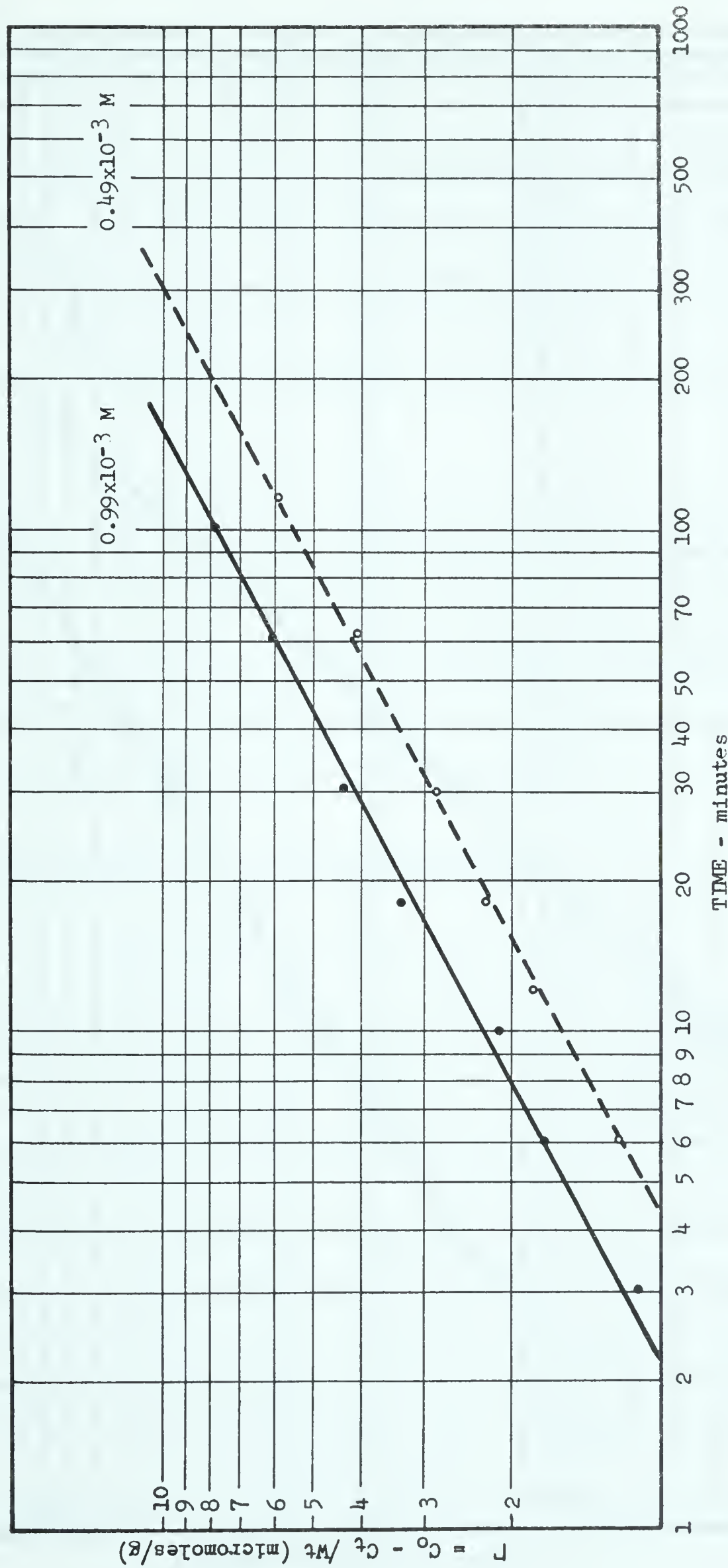


FIG. 14 - EFFECT OF A CHANGE IN XANTHATE CONCENTRATION ON ADSORPTION OF KET₃X FROM A SOLUTION OF KET₃X ON LOG OF COPPER (NOT REDUCED) IN A SYSTEM OPEN TO THE ATMOSPHERE AT 100 C.

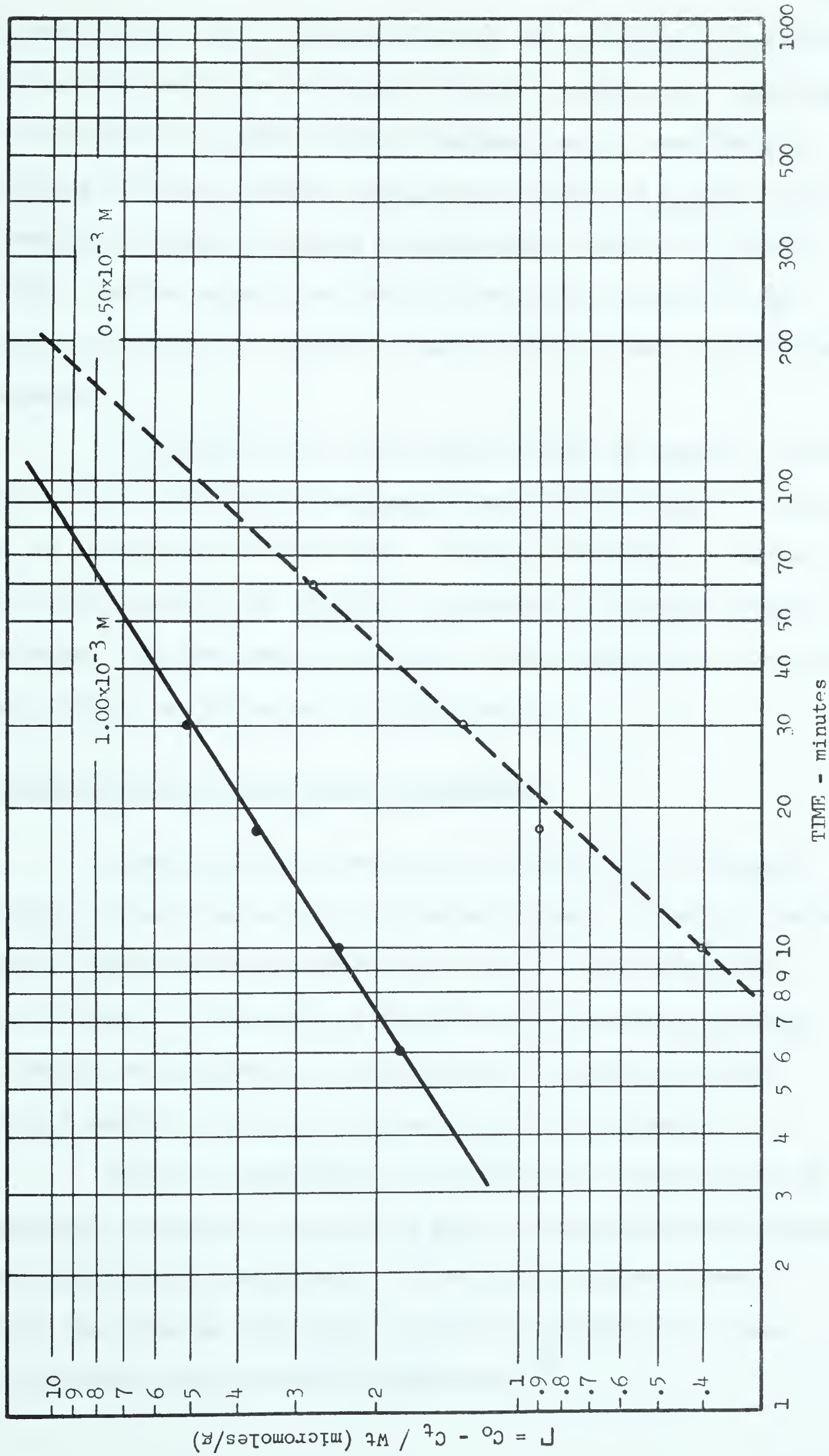


FIG. 15 - EFFECT OF A CHANGE IN XANTHATE CONCENTRATION ON ADSORPTION OF KFtx FROM A MIXTURE OF KFtx AND C₁₂TAB ON 10_f OF COPPER (NOT REDUCED) IN A SYSTEM OPEN TO THE ATMOSPHERE AT 10°C.

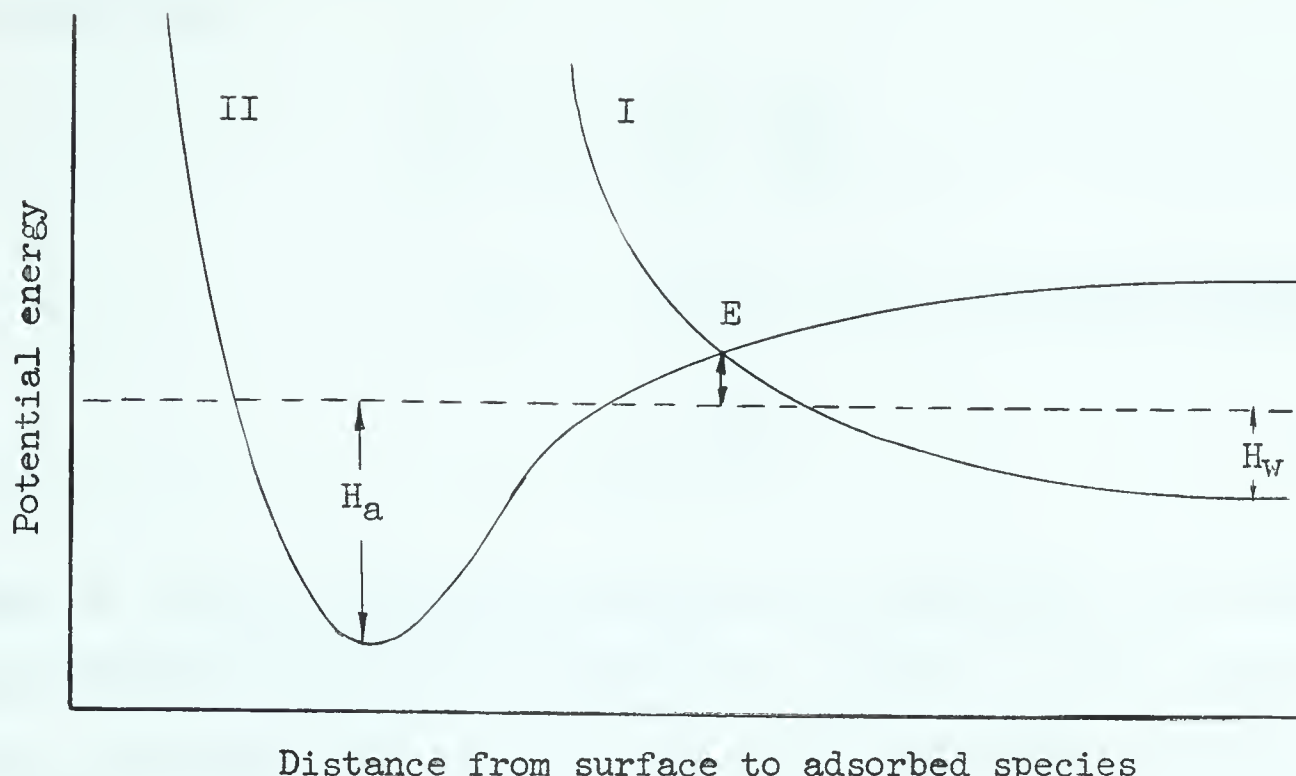
Both results are a good indication that we are dealing with a second order reaction mechanism with respect to the xanthate ion, regardless of the addition of C_{12} TAB. These findings plus the fact that, in some tests with the equimolar combination of KETX and C_{12} TAB, all of the xanthate is removed leaving an appreciable amount of C_{12} TAB in solution, tend to support the idea that the modus operandi of the xanthate abstraction is the same in both cases and that C_{12} TAB is not chemisorbed.

Unfortunately the same analysis cannot be applied to the range of slow abstraction of xanthate because initial concentrations when the break occurs are not known. Graphical evidence is the only proof that a second order reaction is operative in the fast abstraction range. The same graphs indicate also that the reaction rate constants for the two steps have different values.

Activation Energy as a Criterion of Mechanism

Chemisorption is arbitrarily referred to as an adsorption with a molar free energy of attachment around 10 Kcal or greater. Langmuir³¹ emphasized that chemisorption cannot extend beyond the first monolayer. Chemisorption, therefore, is of primary interest in flotation systems because selectivity may be readily obtained through a specific adsorption between collector and mineral.

Physical adsorption, on the contrary, requires little or no activation energy and occurs when there are weak adhesional forces between adsorbate and adsorbent. The difference between chemisorption and physical adsorption is best illustrated by the classical potential energy curve of Lennard-Jones³²:



Physical adsorption is represented by curve I. H_W indicates a small exothermic heat of adsorption, the subscript referring to the van der Waals interactions. Curve II is the classical potential energy curve for a chemically bonded compound. E is the activation energy necessary for chemisorption and H_a is the heat of adsorption of the process. Transition from physical adsorption to chemisorption then takes place through the energy barrier E .

In 1889 Arrhenius proposed an equation relating activation energy to the variation of rate constant with temperature. Starting from the Van't Hoff equation for the temperature co-efficient of the equilibrium constant ($d \ln K/dT = \Delta E/RT^2$) and applying the principle of mass action for the rate constant ($K = k_1/k_{-1}$) he assumed, by analogy, a similar equation:

$$\frac{d \ln k}{dT} = \frac{E_a}{RT^2} \quad (1)$$

On integration:

$$\int d \ln k = \frac{E_a}{R} \int \frac{dT}{T^2}$$

$$\ln k = - \frac{E_a}{RT} + \ln A \text{ (integration constant)}$$

$$k = A e^{-E_a/RT}$$

Where A is the temperature independent pre-exponential factor and E_a the Arrhenius activation energy. This equation, in most cases, gives a straight line if $\ln k$ is plotted against $1/T$. A modified version that accounts for the temperature dependance of A is given by the collision theory of gas reactions. For a second order reaction:

$$\frac{dC}{dt} = k C_1 C_2$$

$$C = \text{concentration in moles/l} = \frac{10^3 N}{L}$$

Where L is the Avogadro's number and N the number of molecules/cc ther.

$$\frac{dC}{dt} = \frac{10^3}{L} \frac{dN}{dt}$$

Therefore:

$$\frac{10^3}{L} \frac{dN}{dt} = k \left(\frac{10^3 N_1}{L} \right) \left(\frac{10^3 N_2}{L} \right)$$

$$k = \frac{L}{10^3 N_1 N_2} \frac{dN}{dt} \quad (2)$$

For a bimolecular reaction, the number of molecules reacting per second

is given by the collision theory as:

No of molecules/cc sec = collision/sec \times fraction of molecules with energy $\geq E$

$$\frac{dN}{dt} = Z_{12} e^{-E/RT}$$

Substituting in (2)

$$k = \frac{L}{10^3 N_1 N_2} Z_{12} e^{-E/RT} \quad (3)$$

but for the case of unlike molecules, the collision frequency Z_{12} , expressed in terms of the mean molecular diameter ($d_{12} = \frac{d_1 + d_2}{2}$) and the reduced mass ($\mu = \frac{m_1 m_2}{m_1 + m_2}$), becomes:

$$Z_{12} = N_1 N_2 d_{12}^2 \sqrt{\frac{8kT}{\pi \mu}}$$

Where k is the Boltzmann constant. Substituting in equation (3):

$$k = \frac{L}{10^3 N_1 N_2} \left(N_1 N_2 d_{12}^2 \sqrt{\frac{8kT}{\pi \mu}} \right) e^{-E/RT}$$

Simplifying and calling A_1 all the pre-exponential terms with the exception of \sqrt{T} :

$$k = A_1 \sqrt{T} e^{-E/RT} \quad (4)$$

The difference between E and E_a can be easily calculated by rewriting equation (4) in a logarithmic form and equating the result to the Arrhenius equation (1):

$$\ln k = \ln A_1 + \frac{1}{2} \ln T - \frac{E}{RT}$$

$$\frac{d \ln k}{dT} = \frac{1}{2T} + \frac{E}{RT^2}$$

$$\frac{1}{2T} + \frac{E}{RT^2} = \frac{E_a}{RT^2}$$

$$E_a = E + \frac{1}{2} RT$$

Therefore the Arrhenius equation is not temperature independent but the correction is so small that, in actual fact, it hardly affects the linear plot of the $\ln k$ vs. $1/T$.

It is found that the activation energy varies with temperature, the overall rate constant may well be subdivided between the rate constants for the individual steps. Salomaa³³, investigating the acid-catalyzed solvolysis of esters, noticed that a plot of $\ln k$ vs. $1/T$ departed from linearity especially at very low temperatures. The postulate of two mechanisms followed from an analysis of the rate constant:

$$k = k_1 + k_2 = A_1 \sqrt{T} e^{-E_1/RT} + A_2 \sqrt{T} e^{-E_2/RT}$$

The overall rate constant is the sum of the rate constants for each mechanism. "Chemically"³⁴ this means that some reactant or intermediate

is effectively partitioned between two different reaction pathways".

Fig. 18 indicates that the Arrhenius activation energy is temperature independent suggesting that there is only one rate constant for the process. This is apparently so for an abstraction of xanthate from a solution of xanthate alone (line A in Fig. 18) that is 20% completed

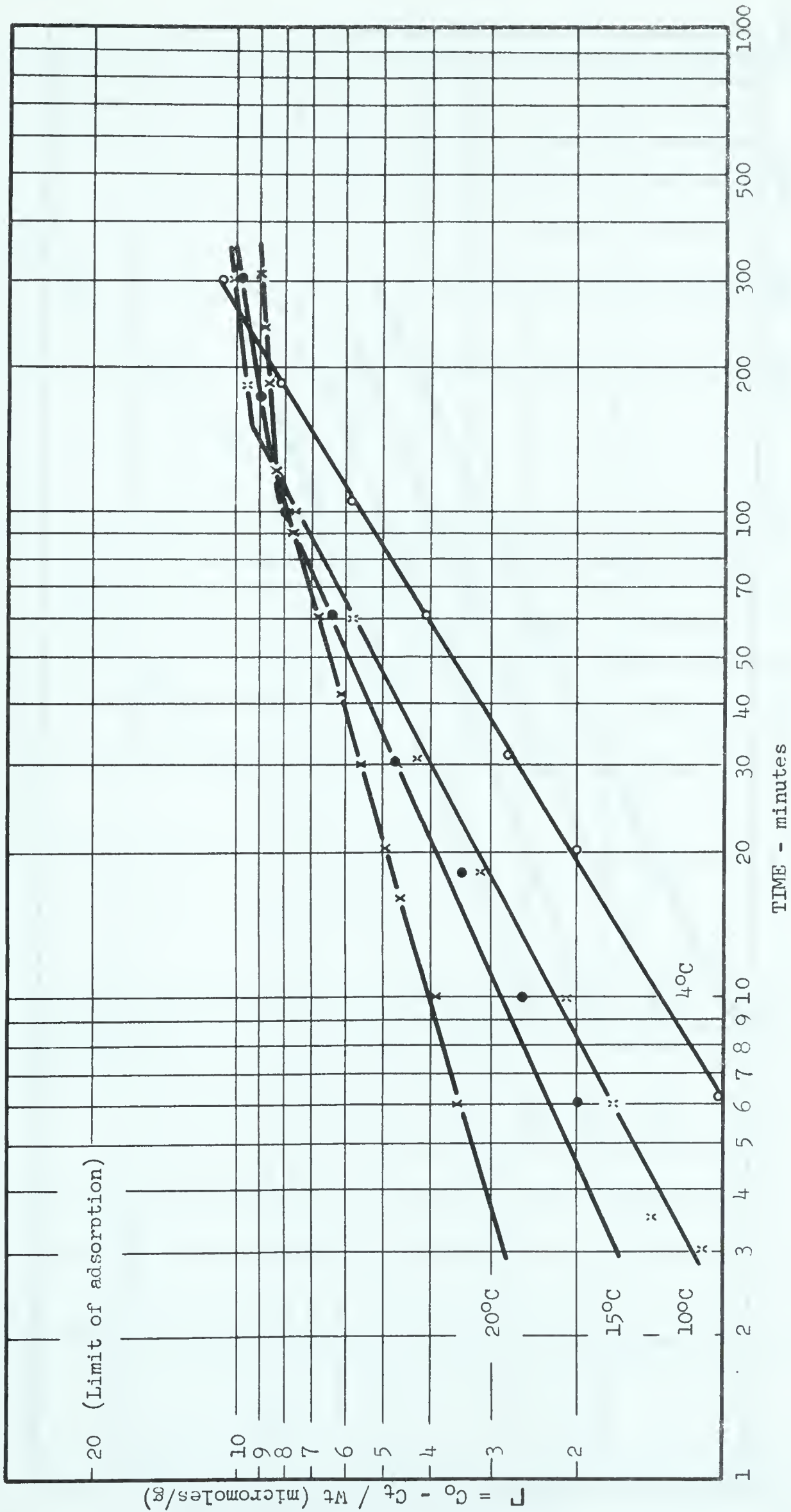


FIG. 16 - ADSORPTION OF KETX ON \log OF COPPER (NOT REDUCED) FROM A SOLUTION OF KETX IN A SYSTEM OPEN TO THE ATMOSPHERE.

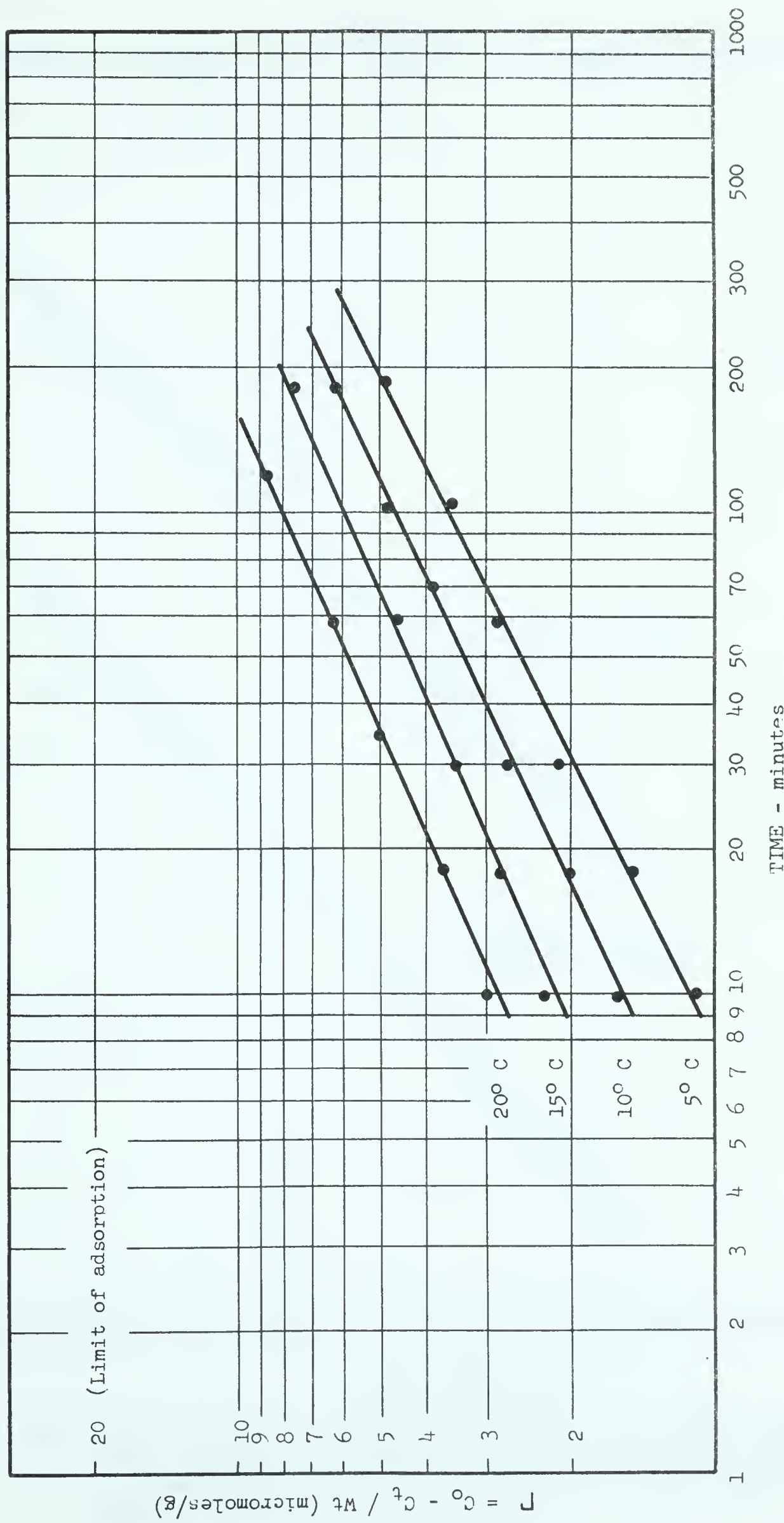


FIG. 17 - ADSORPTION OF KETX ON 10g OF COPPER (REDUCED) FROM A MIXTURE OF KETX AND C₁₂TAB IN A NITROGEN ATMOSPHERE.

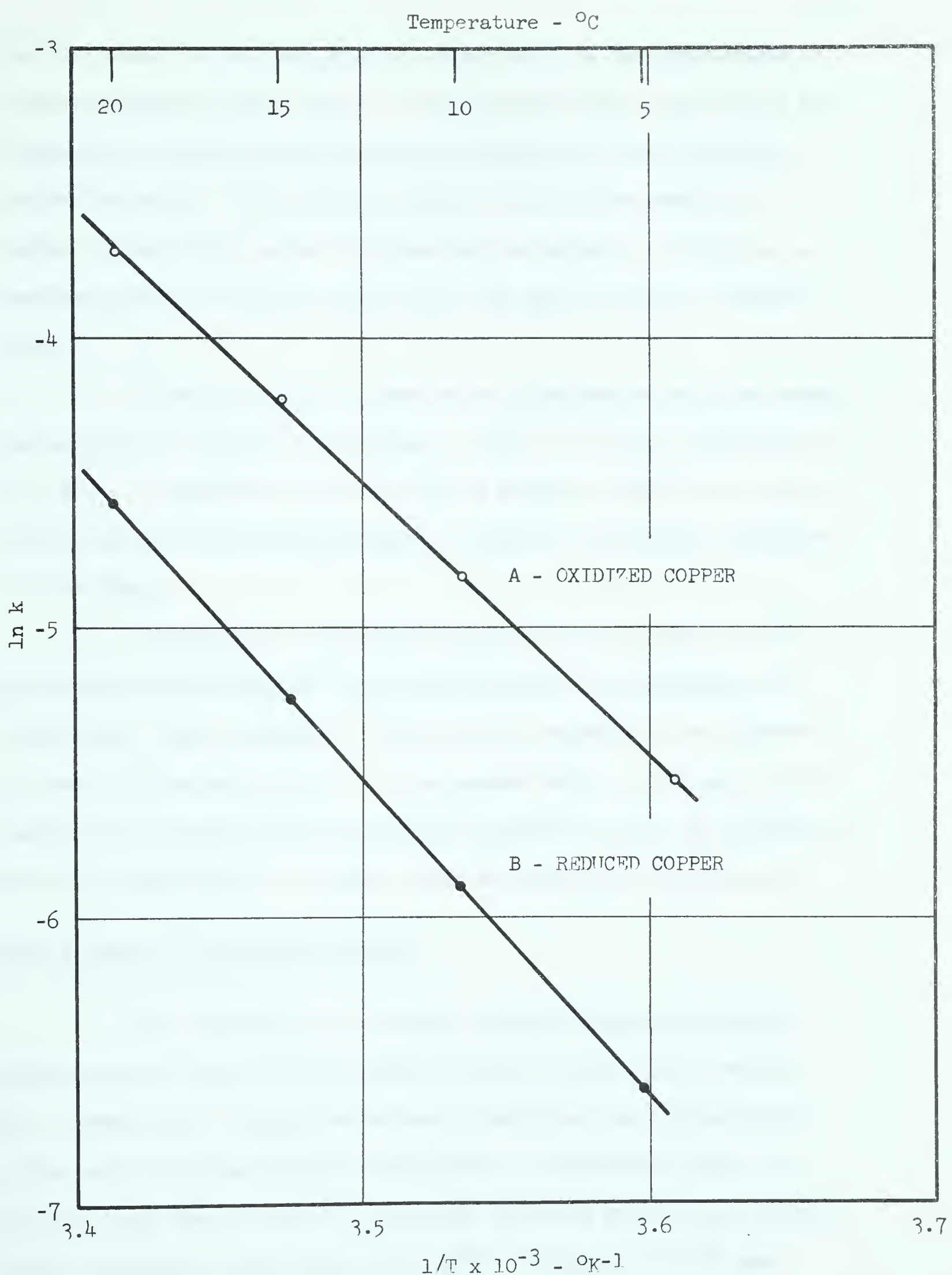


FIG. 18 - TEMPERATURE INDEPENDENCE OF ARRHENIUS ACTIVATION ENERGY FOR KETX FROM A SOLUTION OF KETX ALONE IN A SYSTEM OPEN TO THE ATMOSPHERE (A) AND FROM AN EQUIIMOTAR SOLUTION OF KETX AND C_{12}TAB IN A NITROGEN ATMOSPHERE (B).

but, if higher percentages are used the points on the graph begin to spread suggesting that a series of more sophisticated experiments are required to establish the temperature dependence of the Arrhenius activation energy. The oxidized state of the copper surface is obviously one of the major variables and the extent of oxidation has been impossible to control when copper was used in the "as received" form.

When KETX alone is used as an adsorbate on oxidized copper, the activation energy corresponding to tests in the open atmosphere is 18.3 Kcal. When KETX is adsorbed from a mixture of KETX and $C_{12}TAB$, the activation energy corresponding to tests in a nitrogen atmosphere is 22.6 Kcal.

Entropies of activation have been used by Long et al³⁵ for several acid-catalyzed reactions for which the mechanisms are well known. They demonstrated that the two mechanisms are separated by some 25-30 entropy units. In the present work a difference of 12 entropy units between the two systems described in Fig. 18 (Appendix C) may not be sufficient to suggest that two mechanisms are operative.

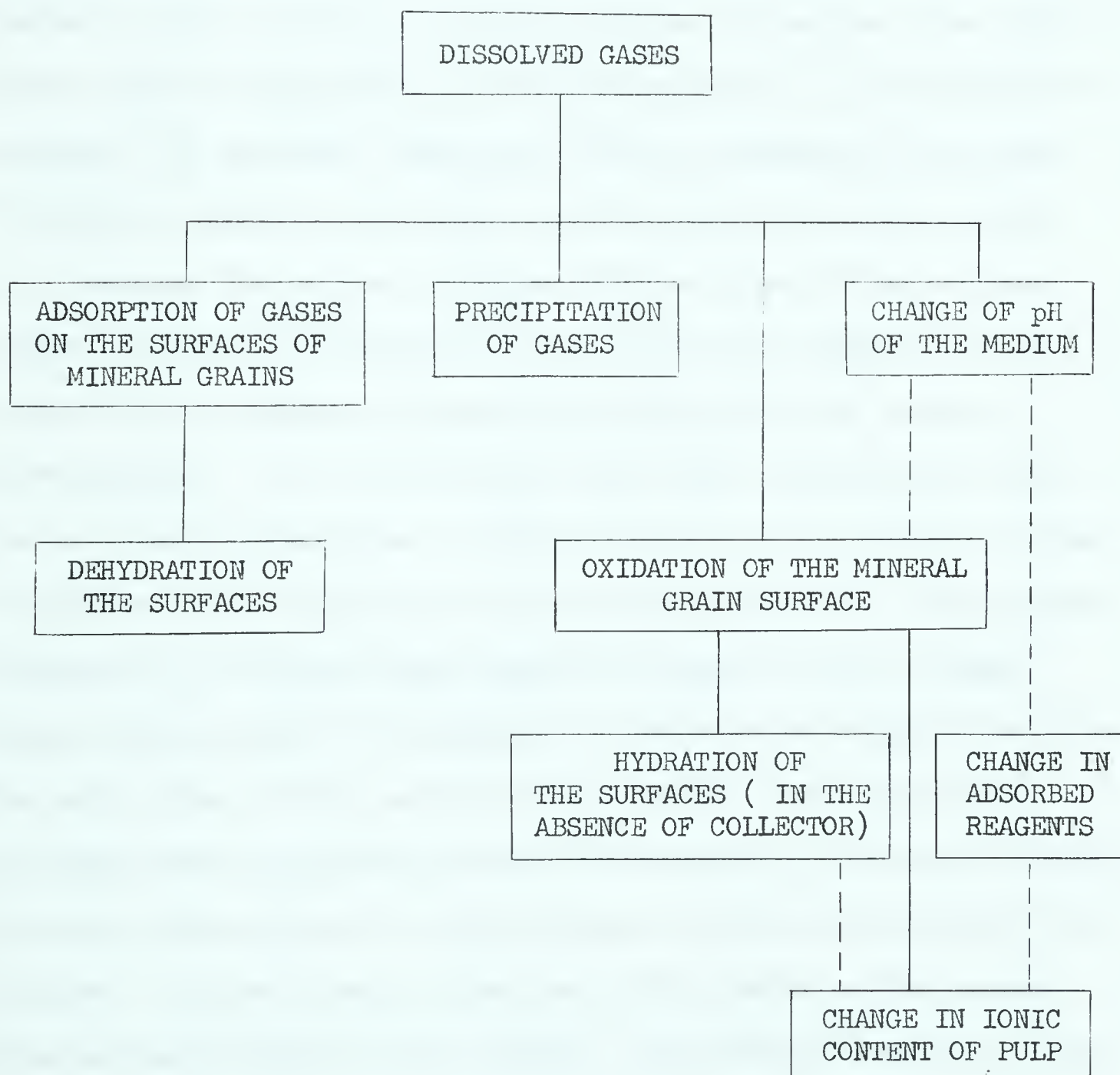
Role of Gases in Adsorption Studies

The hydration of a mineral surface depends on chemical species involved and on the crystal structure which in turn decide the cleavage face. Crystal structure establishes the charge distribution while cleavage reflects the number of unsatisfied bonds. It follows, then that a surface is strongly hydrated when strong electrostatic forces are produced on cleaving^{36a}. Plaksin et al^{36b} have

shown that "adsorption of gases considerably lowers the hydration of surfaces of minerals and metals". Adsorption of oxygen (in contrast to nitrogen) aids the interaction of collectors (tall oils) with phosphorites also increasing the hydrophobicity of minerals in the absence of collectors. Poling² describes the action of oxygen as a necessary step to oxidize xanthate to dixanthogen but this step is no longer necessary with collectors such as tall oils. In a general way, the effects of dissolved gases in flotation can be summarized as in Table VI.

Figures 3 and 4 show that there is more adsorption of KETX on oxidized than reduced copper indicating that oxidation of the mineral grain surface is more important than the adsorption of gases on the surfaces of mineral grains. These graphs also point out that there is a time delay, longer than 5 hours, necessary to reach the equilibrium state of oxidation existing in the open atmosphere. Plaksin et al^{36c} have shown that different gases (oxygen, nitrogen and carbon dioxide) affect the hydration of metals, sulphides and non-sulphides differently: "The data show that the hydration of the surfaces of noble metals, after contact with gases, is lowered and that oxygen is the most active of the three gases mentioned. Oxygen shows a similar action on the surfaces of sulphide minerals. Nitrogen and carbon dioxide affect minerals to a lesser extent. The same applies to the effect of gases on the hydration of surfaces of non-sulphide minerals and coals". Their investigations on the effect of dissolved oxygen on the interactions with surfactants have indicated that sulphide minerals adsorb a considerable

TABLE VI - GENERAL SCHEME OF INFLUENCE OF DISSOLVED GASES ON FLOTATION
 (from "An Introduction to the Theory of Flotation" by V. I. Klassen and V.A. Mokrousov).



amount of oxygen from water and that these minerals do not interact with xanthates if there is no oxygen in the water. "However, different concentrations of oxygen are required for optimum floatability of different minerals".^{36c} Moreover, "it has been established that oxygen dissolved in the pulp improved the interaction of collectors not only with sulphides but also with non-sulphide minerals with all anionic collectors. Experimental confirmation of this was completely unexpected".^{36c} According to Klassen^{36d} "oxygen, dissolved in water, adsorbs on mineral surfaces better than other gases. Three stages of adsorption can be distinguished: (1) reversible adsorption, (2) activated adsorption with the attachment of molecules or atoms of oxygen to the surface and (3) oxidation of the surface, i.e. chemical interaction of oxygen with the atoms of the surface layer." Plaksin and Bessonov^{36d} have added that "chemisorption of oxygen without immediate chemical interaction with the surface is also possible." It is obvious then that before chemisorption there is an activated adsorption of oxygen molecules on the surface causing a decrease in the hydration of the surface in question. The improved adsorption of collectors when oxygen is present is due to oxygen which helps not only the adsorption of xanthates on sulphides but also the adsorption of fatty acids on non-sulphides. "One hypothesis is the penetration of oxygen into the surface layer of the mineral weakens the bond between these ions and increases the chemical activity of the surface. In other words, ionization of the mineral surface occurs. This can be attributed to two causes: (1) increased mobility of ions in the surface layer and also improvement in conditions for their ex-

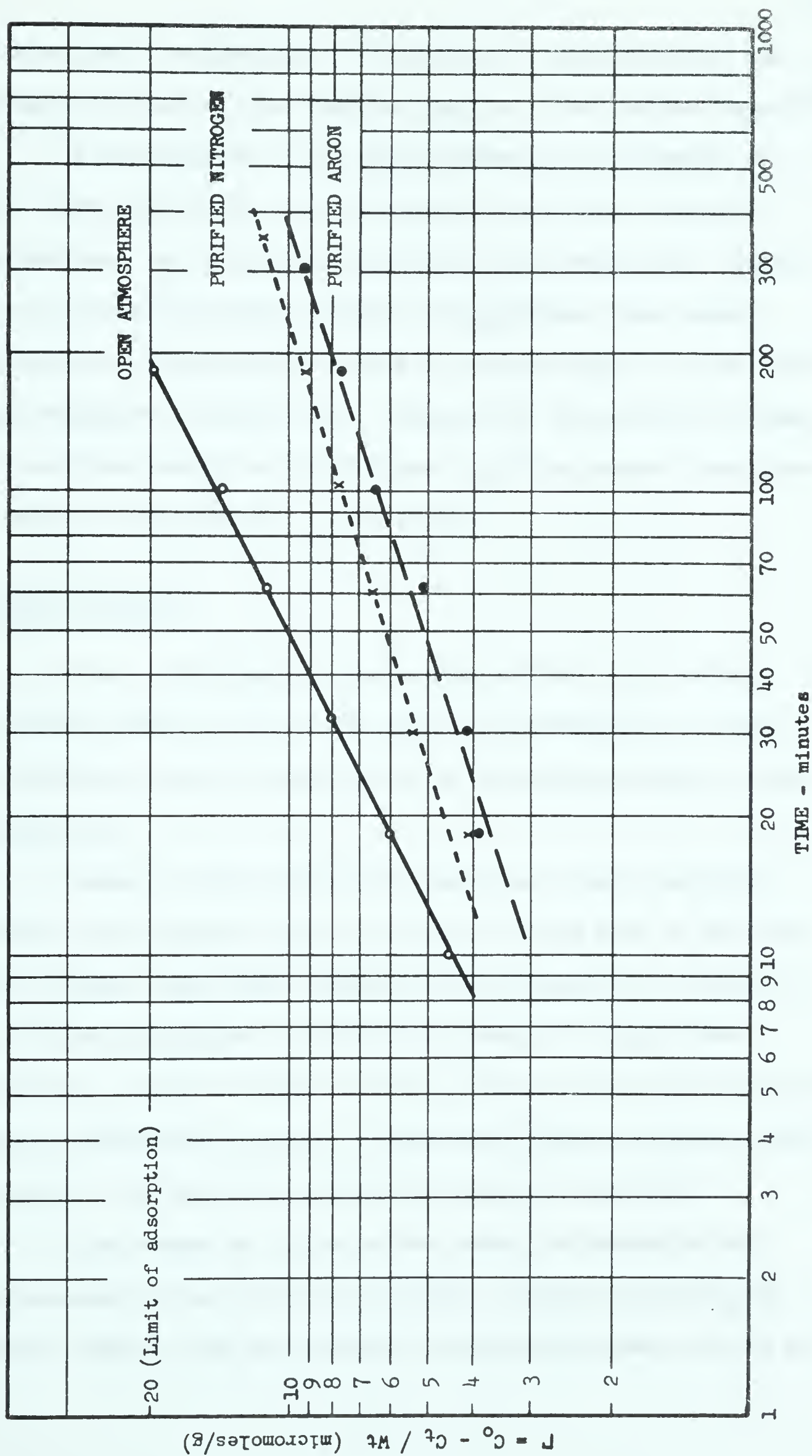


FIG. 19 - INFLUENCE OF VARIOUS GASES ON ADSORPTION OF A MIXTURE OF KETX AND C₁₂TAB ON log OF COPPER (REDUCED) AT 100°C.

change with ions of collectors: (2) creation of conditions for the penetration of collector ions into the lattice of the surface layer."^{36e}

A confirmation of the above statements is presented in Fig. 19. Here, the effect of various gases is not only evident but also proportional to the chemical activity of the gases used. Experiments on an equimolar mixture of KEtX and $C_{12}TAB$ have been chosen because there is no adsorption of KEtX on reduced copper in a purified nitrogen atmosphere (Test No. 53). The point to be noted here is that there is a strong adsorption of KEtX when $C_{12}TAB$ is present regardless of the nature of the gas used in the system.

Evaluation of Results

After collecting and rearranging all the data, certain trends, either common to all of the tests, or pertaining to a fixed set of variables, have been detected as an outstanding feature of the kinetic process.

Common to all tests is the slower and lower adsorption of potassium ethyl xanthate from solutions of either KEtX or KEtX and $C_{12}TAB$ on reduced copper when compared to the adsorption on oxidized copper. Slower adsorption is denoted by a change in slope, lower adsorption by a change in amount adsorbed. There is only one exception: adsorption of KEtX from a mixture of KEtX and $C_{12}TAB$ on reduced or oxidized copper is the same when atmospheric oxygen is available.

Also common to all tests, the amount of potassium ethyl xanthate adsorbed by the substrate is larger and faster when $C_{12}TAB$ is present. This is true for systems in an open atmosphere as well as

for systems under a nitrogen atmosphere, but a preferential adsorption is displayed for the first case when oxygen is present. The converse is also true: a reduction of the oxygen content in solution reduces the adsorption of potassium ethyl xanthate from solutions of KEtX alone as well as from solutions of the mixture of KEtX and C_{12}^{TAB} .

Pertaining to a fixed set of variables is the undetectable adsorption of KEtX on reduced copper powder when oxygen is removed from the system. This lack of adsorption has been recognized long ago but purified nitrogen had to be used in the present work before it could be perceived. For this reason as well as for a difference in surface area one should not compare Fig. 19 to Fig. 4 or Fig. 17 to Fig. 8, and all tests appearing in any one section (e.g. Figs. 16, 17, 19) have been carefully selected or repeated.

A separate and outstanding case is the effect of temperature on the adsorption of potassium ethyl xanthate. When the temperature is lowered, the adsorption is affected in one or more of the following ways: (a) the amount adsorbed is reduced; (b) the transition point from one type of adsorption to another is displaced (e.g. from 150 min. at $10^{\circ}C$ to 30 min at $4^{\circ}C$ for oxidized copper); (c) the rate of adsorption is apparently reversed. While the first two aspects require little attention, the last point demands a proper explanation. What can be referred to as a slow and fast adsorption in Fig. 7 should not be compared to the fast and slow adsorption in Fig. 3. The adsorption of Fig. 1 is very rapid, therefore, if we slow down the process by changing from oxidized to reduced copper, rather than lowering the temperature, the actual steps of adsorption become: slow, fast,

and slow (Fig. 4: adsorption of KETX in a system open to the atmosphere). This sequence now is in perfect agreement with Fig. 7 that, naturally, shows only the slow and fast adsorption steps. Moreover, if we think of a surface in terms of active sites, it is easy to conceive that at a lower temperature the number of active sites must be reduced. Adsorption, then, can be described as consisting of two steps: (1) occupation of the active sites by the surface active agent; (2) build up of xanthate crystallites. The contribution of these steps determines the adsorption rate. At a low temperature the active sites are further apart and once they are occupied (slow adsorption) other sites are activated, thus allowing both steps to occur simultaneously (fast adsorption). Once all of the active and activated sites are taken only the formation of the crystallites remains (final slow step). At 10°C the first slow adsorption step is undetected because it takes place in a very short time (less than 3 minutes). The above sequence is in good agreement with a monolayer coverage (12 micromoles/g) as calculated in Appendix A.

Suggestions for Future Flotation Work

The results obtained in this study may be utilized in subsequent investigations of synthetic and actual flotation systems to evaluate changes in selectivity due to complexes of surface active agents, particularly in systems deficient of oxygen.

SUMMARY AND CONCLUSIONS

When an alkali metal xanthate is dissolved in water it completely dissociates into xanthate anions and metal cations. It is also known that a heavy metal xanthate is formed on the metal surface during adsorption but a large degree of uncertainty remains in establishing the actual reaction path. Another reported fact, here reconfirmed to be true, is that there is no adsorption of a xanthate anion on a clean metal surface from a deoxygenated solution. The presence of a poison or inhibitor, therefore, is necessary for adsorption. To overcome this "adsorption barrier" authors like Cook and Nixon proposed the free acid theory while Poling and Leja suggested dixanthogen as the main adsorbing species. Both theories have a common denominator: a neutral molecule that easily penetrates the diffuse double layer. Following these lines of thought it is logical to conceive that a neutral complex capable of stabilizing xanthate anions could be as effective as the dixanthogen or the xanthic acid previously mentioned.

The experimental data indicate that:

- 1) xanthate anions adsorb faster when $C_{12}TAB$ is present (Figures 3 to 8);
- 2) adsorption of xanthate anions is affected more by the oxygen on the metal surface than by the oxygen in solution (Figures 3 and 4);
- 3) $C_{12}TAB$ carries effectively xanthate anions to the metal surface in the absence of oxygen (Figures 4, 8, 19);
- 4) a change in the type of gas used in the adsorption system

modifies the adsorption characteristics of xanthate anions (Figures 4, 8, 19);

- 5) strong adsorption of xanthate from KEtX + C₁₂TAB mixture occurs with all gases even with an inert one like argon (Figure 19);
- 6) in systems with oxidized copper, the reaction forming the heavy metal xanthate is of the second order with respect to the xanthate anion;
- 7) activation energies vary with different states of surfaces (oxidized and reduced), but their value does not change in the 4° - 20°C range;
- 8) calculated entropies of activation are negative indicating that the reaction between xanthate and metal-containing substrate is of the "slow" type.

On the basis of the evidence presented above, it is concluded that:

- a) the effect of a change in substrate is much more pronounced in adsorption from solutions of KEtX alone than in adsorption from the mixture of KEtX and C₁₂TAB;
- b) adsorption of xanthate anions complexed with C₁₂TAB takes place in absence of oxygen. In other words, oxygen is not a sine qua non condition of xanthate adsorption.

Adsorption of xanthate ions is postulated to occur in three easily recognized steps:

- i) adsorption of collector on the available active sites

present on the copper powder;

- ii) concurrent adsorption on the activated sites and formation of xanthate crystallites;
- iii) limited adsorption on growing multimolecular crystallites of xanthates.

Availability of C_{12}^{TAB} ions in solution facilitates the formation of a neutral xanthate- C_{12}^{TAB} complex that can easily penetrate the Stern double layer present at the solid/liquid interface. Final adsorption is due to the splitting of the weakly bonded complex into ethyl xanthate anions and C_{12}^{TAB} cations and subsequent chemisorption of ethyl xanthate anions. The last step can be explained in terms of relative bond strength. The pyramidal base of the C_{12}^{TAB} cation with the three methyl groups provides a triform resonance hybrid where xanthate anions can attach themselves. In the proximity of the solid/liquid interface, the availability of metal cations and free electrons favours the formation of the strongest bond: chemisorption of xanthate anions. C_{12}^{TAB} cations then are again free to establish a dynamic equilibrium with the solid surface, thus maintaining almost a constant concentration in solution in spite of xanthate chemisorption.

REFERENCES

1. Hagiwara H., J. Phys. Chem. 56, 616 (1952)
2. Poling G.W., Ph.D. Thesis, U. of A., Edmonton (1963)
3. Sheka Z.A. and Kriss E.E., Ukrainian Akad, Nauk, U.S.S.R., p. 135 (1959)
4. Taggart A.F. et al., Trans. AIME, 87, 217 (1934)
5. Sutherland K.L. and Wark I.W., "Principles of Flotation", AIMM, 1955
6. Gaudin A.M., "Flotation", Mc-Graw Hill Book Co. Inc., 1957
7. Cook M.A., Nixon J.C., J. Phys. and Coll. Chem. 54, 445 (1950)
8. Cook M.A., Wadsworth M.E., Proc. 2nd Int. Cong. on Surface Activity, Butterworths, Vol. 3, 228 (1957)
9. Gaudin A.M., Bloecher F.W., Trans. AIME 187, 499 (1950)
10. Fuerstenau D.W., AIME Trans., 208, 1365 (1957)
11. Gaudin A.M., Morrow J.G., AIME Trans., 199, 1197 (1954)
12. Fuerstenau D.W., Modi H.J., N.Y.O. 7178, MITS 31 (1956) and N.Y.O. 7179, MITS 32 (1956), Massachusetts Institute of Technology
13. Purcell G., Ph.D. Thesis, Pennsylvania State University (1960)
14. Helmholtz H., Monats. Preuss. Akad. Sci. (1881); Akad. Ann. 7, 337 (1879)
15. Gouy E., J. Phys., 9, 457 (1910); Ann. Phys., 7, 129 (1917)
16. Chapman D.C., Phil. Mag., 25, 475 (1913)
17. Stern O., Z. Electrochem., 30, 508 (1924)
18. Grahame D.C., Chem. Revs., 41, 441 (1947)
19. Potter E.C., "Electrochemistry", Cleaver-Hume Press Ltd., London, p. 158
20. Moore W., "Physical Chemistry", Prentice-Hall Inc., Englewood Cliffs, 1963
21. Pomianowski A., Leja J., Can. Journal of Chem., 41, 2219 (1963)
22. Pomianowski A., Leja J., Trans. AIME, 229, 307 (1964)

23. Buckenham M.H., Schulman J.H., Trans. AIME, 226, 1 (1963)
24. Bowcott J.E.L., 2nd Int. Cong. of Surf. Act., III, p. 267 (1957)
25. Warren G.G., Matthews F.W., Anal. Chem., vol. 26, No. 12, 1985 (1954)
26. Brock M.J., Hannum M.J., Anal. Chem. vol. 27, No. 9, 1374 (1955)
27. Weissberger, "Technique of Organic Chemistry", Vol. VIII, part II, p. 142 (1963)
28. Sowden R.G., Davidson N., J. Am. Chem. Soc., 78, 1291 (1956)
29. Mulliken R.S., J. Phys. Chem. 56, 801 (1952)
30. Ingold C.K., Proc. Chem. Soc., 279 (1957)
31. Langmuir I., J. Am. Chem. Soc., 40, 1361 (1918)
32. Lennard-Jones J.E., Trans. Faraday Soc., 28, 334 (1932)
33. Salomaa P., Acta Chem. Scand., 11, 239 (1957)
34. Weissberger, "Technique of Organic Chemistry", Vol. VIII, part I, p. 199 (1963)
35. Long F.A., Pritchard J.G., Stafford F.E., J. Am. Chem. Soc., 79, 2362 (1957)
36. Klassen V.I., Mokrousov V.A., "An Introduction to the Theory of Flotation", (a) p. 41, (b) p. 44, (c) p. 208, (d) p. 217, (e) p. 218, Butterworths, London (1963).

APPENDIX A

Surface Area Measurements

Before measuring the actual surface area of the copper powder, the following preliminary investigations were carried out:

- a) The amount of stearic acid chemisorbed by 10g of copper powder was calculated to be in the order of 10^{-5}M for a surface area of approximately $500 \text{ cm}^2/\text{g}$.
- b) The residue of pure heptane (as obtained by drying 10 ml of solution at 90°C) was measured as 0.00008 g/10 ml. All subsequent weights were corrected by this amount.
- c) All of the experiment was performed at 20°C allowing no less than 90 minutes for the solution to reach equilibrium.

Actual measurements of the amount of stearic acid present in solution were made in the following sequence:

- 1) 0.28386g were dissolved in 100 ml of heptane ($0.998 \times 10^{-2} \text{M}$);
- 2) 10 ml of solution (1) were diluted to 100 ml. On evaporation of 10 ml of solution it was found that instead of 0.002838g, 0.002835g ($0.996 \times 10^{-5} \text{M}$) were actually present.
- 3) After adding 10g of copper powder, the amount of stearic acid in solution was 0.000283g/10 ml.

$$\text{Amount adsorbed} = 0.00255 \text{g/g of Cu}$$

- 4) 5 ml of (1) were added (0.01418g) to give a total of 0.04225g ($1.485 \times 10^{-5} \text{M}$) in the 100 ml containing the copper powder. 10 ml of this solution contained 0.001571g of stearic acid.

Amount adsorbed = 0.00265g/g of Cu

5) 5 ml of (1) were added (0.01418g) to give a total of 0.05486g (1.928×10^{-5} M) in the 100 ml containing the copper powder. 10 ml of this solution contained 0.002755g of stearic acid.

Amount adsorbed = 0.00276g/g of Cu

6) 10 ml of (1) were added (0.02835) to give a total of 0.08046g (2.828×10^{-5} M) in the 100 ml containing the copper powder. 10 ml of this solution contained 0.003590g of stearic acid.

Amount adsorbed = 0.004456g/g of Cu

7) 10 ml of (1) were added (0.02835g) to give a total of 0.10522g (3.699×10^{-5} M) in the 100 ml containing the copper powder. 10 ml of this solution contained 0.006020g of stearic acid.

Amount adsorbed = 0.00450g/g of Cu

8) A fresh 10g sample of the copper powder was added to 100 ml containing 0.15740g (5.533×10^{-5} M) of stearic acid. 10 ml of this solution contained 0.015305g of stearic acid.

Amount adsorbed = 0.00435g/g of Cu.

Considering an average saturation adsorption of 0.0045g/g of Cu (Fig. 20), the number of molecules (n) present in this quantity is:

$$n = \frac{0.0045}{284.47} \times 6.02 \times 10^{23}$$

$$= 9.52 \times 10^{18} \text{ molecules}$$

From the given cross-sectional area of the carboxylic acid group ($20.5 \text{ \AA}^2 = 20.5 \times 10^{-16} \text{ cm}^2$), the total area of the 1g sample is:

$$\begin{aligned}\text{Area} &= 20.5 \times 10^{-16} \times 9.52 \times 10^{18} \\ &= 19500 \text{ cm}^2/\text{g} \\ &= 1.95 \text{ m}^2/\text{g}\end{aligned}$$

Then the number (n_1) of xanthate molecules (27 \AA^2) required to form a monolayer is:

$$n_1 = \frac{19.5 \times 10^{19}}{27} = 7.2 \times 10^{18}$$

$$\text{Equivalent molar concentration} = \frac{7.2 \times 10^{18}}{6.0 \times 10^{23}} = 1.2 \times 10^{-5} \text{ M}$$

or 12 micromoles/g.

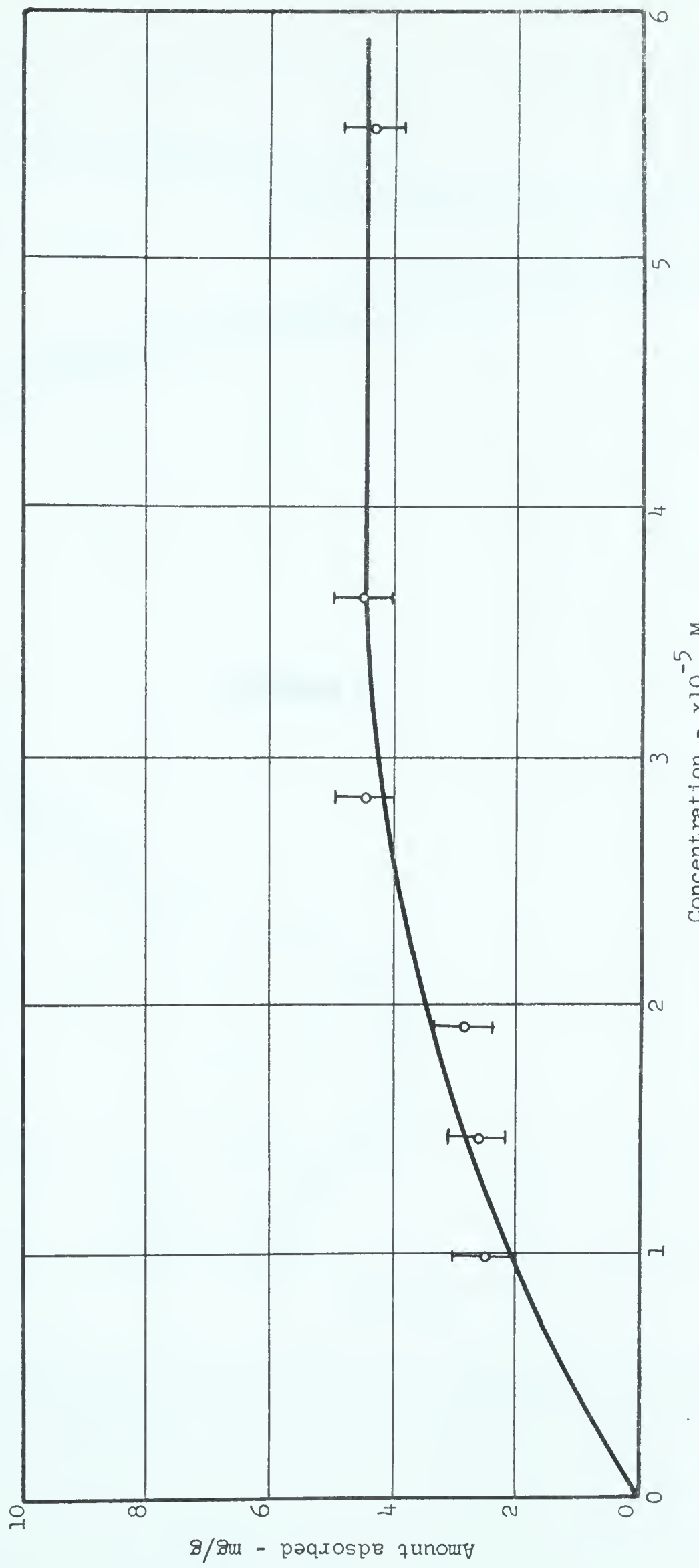


Fig. 20 - ADSORPTION ISOTHERM FOR STEARIC ACID ON COPPER POWDER AT 20°C .

APPENDIX B

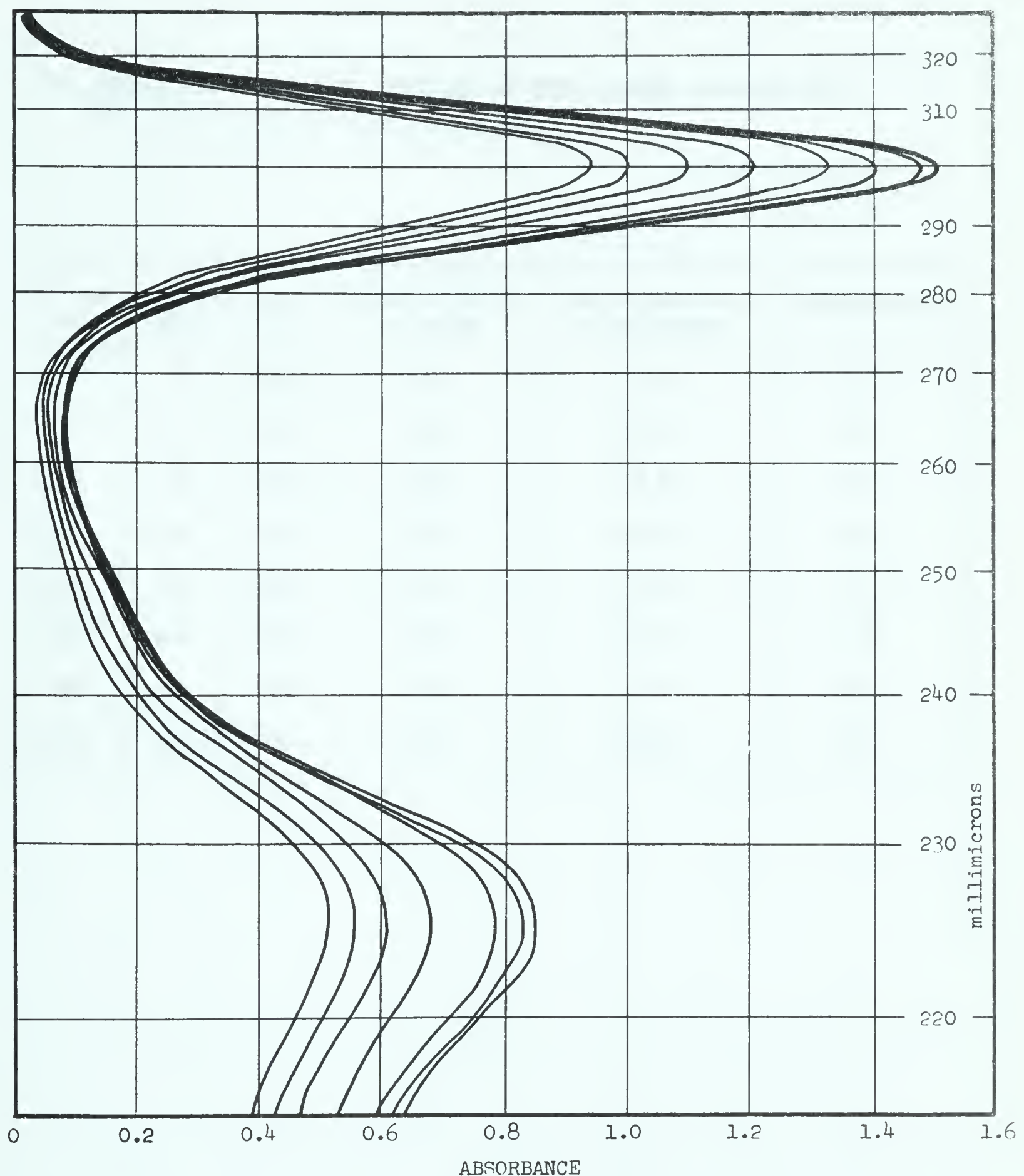


FIG. 21 - TEST NO. 17 - 10g of copper (not reduced) - Nitrogen atmosphere - 10°C
KetX: 1.005×10^{-3} M - 1 mm cell - Resolution: 2 - Scan speed: 4 -
Pen response: 2 - Date of test: September 16, 1964.

TABLE VII - DETAILED ANALYSIS OF TEST NUMBER 17 (Fig. 21).

Volume ml.	Time min.	d_{301}	Concentration $\times 10^{-3}M$	Amount adsorbed $\times 10^{-6}$ moles	Micromoles/g
198	6	1.50	0.94	13.0	1.3
197	10	1.48	0.92	16.7	1.7
196	18	1.40	0.86	28.4	2.8
195	30	1.32	0.80	39.4	3.9
194	60	1.22	0.73	53.3	5.3
193	100	1.10	0.65	68.5	6.8
192	180	1.01	0.59	79.7	8.0
191	300	0.95	0.55	86.9	8.7

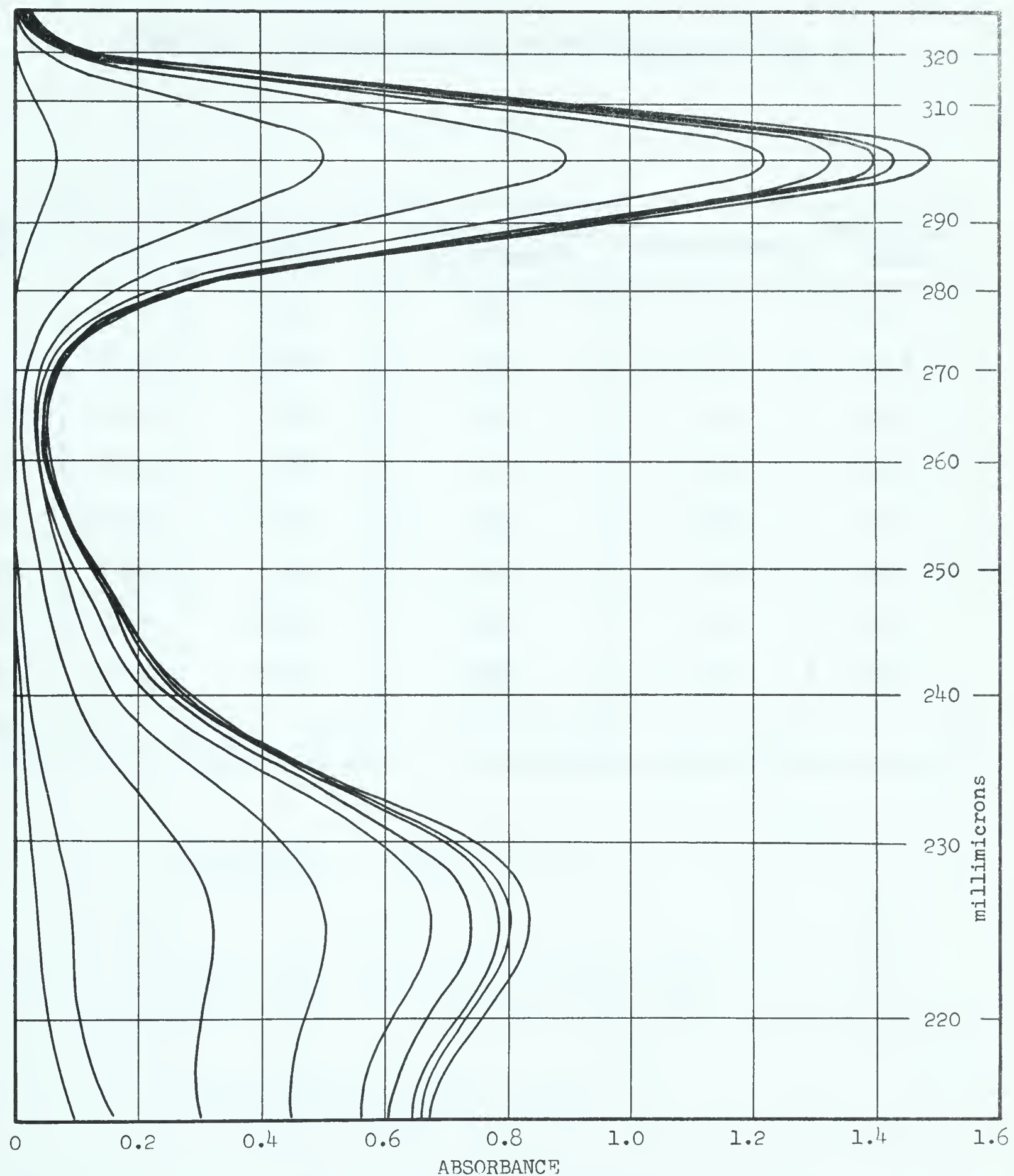


FIG. 22 - TEST NO. 16 - 10g of copper (reduced) - Open atmosphere - 10°C -
KETX: 1.004×10^{-3} M, C_{12}TAR : 1.004×10^{-3} M - 1 mm cell - Resolution: 2
Scan speed: 4 - Pen response: 2 - Date of test: September 14, 1964.

TABLE VIII - DETAILED ANALYSIS OF TEST NUMBER 16 (Fig. 22).

Time min.	d_{301}	Concentration $\times 10^{-3}M$	Amount adsorbed $\times 10^{-6}$ moles	Micromoles/g	Corrected value
3	1.49	0.93	15	1.5	1.4
7	1.43	0.88	25	2.5	2.3
10	1.40	0.85	35	3.5	3.3
18	1.33	0.80	41	4.1	3.9
30	1.22	0.73	55	5.5	5.2
60	0.89	0.52	97	9.7	9.4
100	0.50	0.28	145	14.5	14.1
180	0.07	0.04	200	20.0	19.3
300	-	-	-	-	-

Least square analysis of test number 16.

$y = \text{moles/g}$	$x = \text{time}$	$Y = \ln y$	$X = \ln x$	XY	x^2	y^2
1.4	3	0.34	1.10	0.37	1.21	0.11
2.3	7	0.83	1.95	1.62	3.80	0.69
3.3	10	1.19	2.30	2.74	5.29	1.42
3.9	18	1.36	2.89	3.93	8.35	1.85
5.2	30	1.65	3.40	5.61	11.56	2.72
9.4	60	2.24	4.09	9.16	16.73	5.02
14.3	100	2.66	4.60	12.24	21.16	7.07
19.3	180	2.96	5.19	15.36	26.94	8.76
-	-	13.23	25.52	51.03	95.04	27.64

$$\text{intercept} = \frac{\sum x^2 \sum y - \sum xy \sum x}{N \sum x^2 - (\sum x)^2} = \frac{95.04 \times 13.23 - 25.52 \times 51.03}{8 \times 95.04 - (25.52)^2}$$

$$= \frac{1257 - 1302}{760.3 - 651.3} = \frac{-45}{109.0} = -0.41$$

$$\text{slope} = \frac{N \sum xy - \sum x \sum y}{N \sum x^2 - (\sum x)^2} = \frac{8 \times 51.03 - 25.52 \times 13.23}{8 \times 95.04 - (25.52)^2}$$

$$= \frac{408.2 - 337.6}{109.0} = \frac{70.6}{109.0} = 0.65$$

From Figure 4 it appears that there is a variation of ± 0.2 micromoles at 3 minutes, ± 0.4 micromoles at 10 minutes, and ± 1.5 micromoles at 100 minutes. This discrepancy is inherent in the least square analysis

since equal weights are placed on every value

Standard Deviation (Standard Error)

The following estimates are considered to be within a 95.45% confidence limit:

Values affecting X: Time: ± 5 sec = ± 0.08 min.

Values affecting Y: Volume: ± 0.2 ml

Absorbance: ± 0.01 optical units

Concentration: $\pm 0.1 \times 10^{-4}$

Since there are four standard deviations (σ_s) in a 95.45% confidence interval, the standard deviation can be derived from a proper analysis of each independent variable.

Time: Variations in time have been considered negligible for the following reasons: (a) least square analysis offers the most likely value of Y only for a given value of X ($X = \ln$ time); (b) impossibility of plotting 0.08 min. on the graphs

Volume: $4\sigma_a = 2 \times 0.2 = 0.4$

$$\sigma_a = 0.1$$

$$\sigma_a^2 = 0.01$$

Absorbance: $4\sigma_b = 2 \times 0.01 = 0.02$

$$\sigma_b = 0.005$$

$$\sigma_b^2 = 25 \times 10^{-6}$$

Concentration: $4\sigma_c = 2 \times 0.1 \times 10^{-4} = 0.2 \times 10^{-4}$

$$\sigma_c = 5 \times 10^{-6}$$

$$\begin{aligned}
 \sum \sigma_c^2 &= 25 \times 10^{-12} \\
 \sigma_s^2 &= \sigma_a^2 + \sigma_b^2 + \sigma_c^2 \\
 &= 0.01 + 25 \times 10^{-6} + 25 \times 10^{-12} \\
 &\approx 0.01 \\
 \sigma_s &= \text{standard deviation} = 0.1
 \end{aligned}$$

The 95.45% confidence limit is:

$$4\sigma_s = 4 \times 0.1 = 0.4$$

Therefore all readings are ± 0.2 micromoles. This value is exactly the same as the value previously observed in the least square analysis at the 3 minute mark.

APPENDIX C

ACTIVATION ENERGY

I - KEtX - Atmospheric Oxygen Present

Time required to complete 20% of the abstraction (Fig. 16)

minutes	9.2	15	28	57
temperature - $^{\circ}\text{C}$	20	15	10	4

$$-\frac{dC}{dt} = kC \quad \text{or} \quad k = \ln \frac{C_0}{C} \frac{1}{t}$$

$$k_1 = (\ln \frac{100}{80}) \frac{1}{9.2} = \frac{0.223}{9.2} = 0.0242 \quad \ln k_1 = -3.72$$

$$k_2 = (\ln \frac{100}{80}) \frac{1}{15} = \frac{0.223}{15} = 0.0149 \quad \ln k_2 = -4.21$$

$$k_3 = (\ln \frac{100}{80}) \frac{1}{28} = \frac{0.223}{28} = 0.00796 \quad \ln k_3 = -4.84$$

$$k_4 = (\ln \frac{100}{80}) \frac{1}{57} = \frac{0.223}{57} = 0.00391 \quad \ln k_4 = -5.54$$

$$20^{\circ}\text{C} = 293^{\circ}\text{K}$$

$$1/293^{\circ}\text{K} = 3.413 \times 10^{-3}$$

$$15^{\circ}\text{C} = 288^{\circ}\text{K}$$

$$1/288^{\circ}\text{K} = 3.472 \times 10^{-3}$$

$$10^{\circ}\text{C} = 283^{\circ}\text{K}$$

$$1/283^{\circ}\text{K} = 3.533 \times 10^{-3}$$

$$4^{\circ}\text{C} = 277^{\circ}\text{K}$$

$$1/277^{\circ}\text{K} = 3.610 \times 10^{-3}$$

$$k = A \sqrt{T} e^{-E/RT}$$

$$\ln k = \ln A + \frac{1}{2} \ln T - E/RT$$

from Fig. 16:

$$\begin{aligned}
 E &= \frac{(5.54 - 3.72) R}{(3.610 - 3.413) \times 10^{-3}} \\
 &= \frac{1.82 \times 1.986 \times 10^3}{0.197} \\
 &= 18.3 \text{ Kcal}
 \end{aligned}$$

II - Equimolar Mixture of KEtX and C₁₂TAB - Nitrogen Atmosphere

Time required to complete 20% of the abstraction (Fig. 17)

minutes	23	42	80	138
temperature - °C	20	15	10	5

$$k_1 = (\ln \frac{100}{80}) \frac{1}{23} = 0.0097 \quad \ln k_1 = -4.54$$

$$k_2 = (\ln \frac{100}{80}) \frac{1}{42} = 0.00531 \quad \ln k_2 = -5.24$$

$$k_3 = (\ln \frac{100}{80}) \frac{1}{80} = 0.00279 \quad \ln k_3 = -5.90$$

$$k_4 = (\ln \frac{100}{80}) \frac{1}{138} = 0.00161 \quad \ln k_4 = -6.64$$

$$E = \frac{(6.64 - 4.54) R}{(3.597 - 3.413) \times 10^{-3}} = 22.6 \text{ Kcal}$$

ENTROPIES OF ACTIVATION

From transition state theory, the rate of reaction (k_1) expressed in terms of the equilibrium constant K^\ddagger is given as:

$$k_1 = \left(\frac{kT}{h}\right) K^\ddagger \quad (a)$$

Expressing K^\ddagger in terms of the free energy of activation in the standard state (ΔF^\ddagger):

$$-\Delta F^\ddagger = RT \ln K^\ddagger$$

$$K^\ddagger = e^{-\Delta F^\ddagger/RT}$$

but

$$\Delta F^\ddagger = \Delta H^\ddagger - T\Delta S^\ddagger$$

therefore

$$K^\ddagger = e^{-\Delta H^\ddagger/RT} e^{\Delta S^\ddagger/T}$$

Where ΔS^\ddagger and ΔH^\ddagger are, respectively, the entropy and enthalpy of activation. Substituting in (a)

$$k_1 = \frac{kT}{h} e^{\Delta S^\ddagger/R} e^{-\Delta H^\ddagger/RT}$$

Since the difference between E_a and ΔH^\ddagger is small³³ ($E_a = \Delta H^\ddagger + RT$ where $RT \approx 600$ calories around room temperature) the expression becomes:

$$\begin{aligned} k_1 &= \frac{kT}{h} e^{\Delta S^\ddagger/R} e^{-(E_a-RT)/RT} \\ &= \left(e \frac{kT}{h}\right) e^{\Delta S^\ddagger/R} e^{-E_a/RT} \end{aligned}$$

Taking common logarithms:

$$2.303 \log k_1 = 2.303 \log \left(\frac{ek}{h}\right) + 2.303 \log T + \Delta S^\ddagger/R - E_a/RT$$

Rearranging:

$$\begin{aligned}\Delta S^\ddagger &= (2.303R) \left(\log k_1 - \log \frac{ek}{h} - \log T + \frac{E_a}{2.303 RT} \right) \\ &= 4.576 \left(\log k_1 - \log \frac{2.718 \times 1.38 \times 10^{-16}}{6.62 \times 10^{-27}} - \log T + \frac{E_a}{4.576 T} \right)\end{aligned}$$

If ΔS^\ddagger is positive, the reaction will be "normal" or "fast", if negative, collision theory indicates that the reaction is a "slow" one. This equation is valid only if k_1 is based on the second as the unit of time, E_a in calories and R in calories/degree mole.

At 20°C (293°K) with an Arrhenius activation energy of 18300 calories (System A of Fig. 18), ΔS^\ddagger is:

$$k_1 = \left(\ln \frac{100}{80} - \frac{1}{552} \right) = \frac{0.223}{552} = 0.000404 \quad \log k_1 = 4.606$$

$$\Delta S^\ddagger = 4.576 (4.606 - 10.753 - 2.467 + 18300/4.576 \times 293)$$

$$= 4.576 (-3.394 - 10.753 - 2.467 + 13.65)$$

$$= -13.55 \text{ cal/degree mole}$$

At 20°C (293°K) with an Arrhenius activation energy of 22600 calories (System B of Fig. 18), ΔS^\ddagger is:

$$k_1 = \left(\ln \frac{100}{80} \right) \frac{1}{1380} = \frac{0.223}{1380} = 0.0001615 \quad \log k_1 = 4.208$$

$$\begin{aligned}\Delta S^\ddagger &= 4.576 (4.208 - 10.753 - 2.467 + 22600/4.576 \times 293) \\ &= 4.576 (-3.792 - 10.753 - 2.467 + 16.85) \\ &= -0.73 \text{ calories/degree mole}\end{aligned}$$

The difference between the two systems is of the order of 12 entropy units and the reaction is a "slow" one. Further work using the same substrate (e.g. dixanthogen on reduced copper in a nitrogen atmosphere) might elucidate the mechanism through a process of elimination.

B29829